

Distance Assisted Recursive Testing

Xuechan Li* Anthony D. Sung† Jichun Xie ‡

September 28, 2021

Abstract

In many applications, a large number of features are collected with the goal to identify a few important ones among them. Sometimes, these features lie in a metric space with a known distance matrix, which partially reflects their co-importance pattern. Proper use of the distance matrix will boost the power of identifying important features. Hence, we develop a new multiple testing framework named the Distance Assisted Recursive Testing (DART). DART has two stages. In stage 1, we transform the distance matrix into an aggregation tree, where each node represents a set of features. In stage 2, based on the aggregation tree, we set up dynamic node hypotheses and perform multiple testing on the tree. All rejections are mapped back to the features. Under mild assumptions, the false discovery proportion of DART converges to the desired level in high probability converging to one. We illustrate by theory and simulations that DART has superior performance under various models compared to the existing methods. We applied DART to a clinical trial in the allogeneic stem cell transplantation study to identify the gut microbiota whose abundance will be impacted by the after-transplant care.

Keywords: Multiple testing, aggregation tree, false discovery proportion (FDP), auxiliary information

*Xuechan Li is a PhD candidate of Biostatistics at Duke University.

†Anthony D. Sung is an Assistant Professor of Medicine at Duke University.

‡Jichun Xie is an Associate Professor of Biostatistics and Bioinformatics at Duke University.

1 Introduction

A typical multiple testing problem aims to identify a small number of important features among many with a controlled false discovery rate. Sometimes, these features lie in a metric space with known pairwise distances. For example, in neuro-imaging studies, the distance between two neurons can be calculated based on their 3D location and the brain anatomy structure; in microbiome studies, the distance between any two amplicon sequence variants (ASVs) can be calculated based on their evolutionary distance; and in spatial analysis, the Euclidean distances between two sites can be calculated via their geometric locations. In these examples, neurons, ASVs, and geometric locations are features of interest. Very often, important features tend to cluster with each other. If two features are close in distance, they are likely to be co-important or co-unimportant. For example, in microbiome studies, two evolutionarily close ASVs often perform similar biological functions. If one is important, the other is probably important too. Thus when testing the ASV abundance association with the treatment, if we can properly incorporate their evolutionary distance, the testing power will be boosted. In this paper, we will develop a new multiple testing method which incorporates the distance information to boost the testing power while controlling the asymptotic feature-level FDR.

Some existing literature provides alternative solutions to incorporate distance information into testing. One of them is to model the features by hidden Markov chains (Sun and Cai, 2009) or hidden Markov random fields (Liu et al., 2012; Shu et al., 2015; Lee and Lee, 2016). The co-importance patterns are introduced by the transition probabilities between the importance and unimportance status among those features. The challenge lies in how to accurately inferring the transition probabilities. Even assuming all the feature statistics follow multivariate Gaussian distribution, it is still hard to derive consistent transition probability estimators without additional information. Another solution is to use the weighted or smoothed P-values in the neighborhood. Zhang et al. (2011) developed a method called FDR_L . FDR_L pre-specified a smoothing window. For each hypothesis, it smooths the p-value across its local neigh-

bors within the window. Recently, Cai et al. (2020) developed a locally-adaptive weighting and screening method named LAWS. LAWS weighted the P-value using the estimated local sparsity level, which is calculated based on a pre-specified kernel function. However, the performance of LAWS heavily depends on the accuracy in local sparsity level estimation, while accurately estimating the local sparsity level is challenging without additional information. In addition, LAWS focuses on a setting that the features are located in a regular lattice and require a non-vanishing proportion of important features. These conditions might not hold for many large-scale feature selection problems.

In this paper, we propose a new solution called Distance Assisted Recursive Testing (DART). It embeds multiple testing into an aggregation tree built upon the feature distances. DART has two stages.

- Stage I is to construct an aggregation tree based on the distance matrix. First, on layer 1, each node contains only one feature; it is also called a leaf. On layer ℓ ($\ell \geq 2$), we gradually aggregate the close child nodes from the previous layers to form new nodes on the current layer. The detailed algorithm is described in Section 2.2.1.
- Stage II is to perform multiple testing (of testing feature importance) on the aggregation tree from Stage I. On layer 1, we apply the multiple testing procedure to asymptotically control the feature-level FDR. Traditional multiple testing method will stop after one-layer of testing but DART will not. On layer ℓ ($\ell \geq 2$), the already-rejected child nodes from the previous layers will be excluded from the nodes on the current layer to form dynamic working nodes. Next, we apply the new multiple testing procedure on the working nodes to control the node-level FDR up to layer ℓ . If a node on layer ℓ is rejected then all its containing features will be rejected. This rejection rule is very aggressive but the feature-level FDR will still be asymptotically controlled under mild conditions (See Section 3). The detailed algorithm is described in Section 2.2.2.

The underlying logic of DART lies in the assumption that closer features are more likely to have co-importance or co-unimportance patterns. Some important features could have weak signal-

to-noise ratios. If one such feature stands alone, its chance to be discovered is hampered by the weak signal-to-noise ratios; if several such features are aggregated, their collective signal-to-noise ratios will be amplified, and thus their chances to be discovered are boosted.

Generally speaking, DART is a hierarchical multiple testing procedure. Some other multiple testing methods also have hierarchical or graphical structures. Goeman and Finos (2012) and Meijer and Goeman (2015) developed the FWER controlling procedures on the trees and directed acyclic graphs. Dmitrienko and Tamhane (2013) developed methods testing hierarchically ordered hypotheses with applications to clinical trials and control FWER. Yekutieli (2008) considers the case when all the original hypotheses represent a node on the tree and develop a method to test those hypotheses simultaneously. Their parent-node P-values are independent from the child node P-values, very different from our model. Guo et al. (2018) developed a per-family error rate (PFER) and FDR controlling procedure for hypotheses with a DAG structure. Soriano and Ma (2017) develops a up-down testing procedure embedded in the partition tree to asymptotically controls node-level FDR for all nodes on the tree. Li et al. (2020) developed a bottom-up multiple testing approach embedded in the aggregation tree.

Although some existing hierarchical multiple testing procedures share some similarities with DART, their settings and focuses are very different. For example, the existing testing methods often assume the tree structure among nodes are known and static, the node P-values follow $\text{Unif}(0, 1)$ under the null, and aims to control node-level FDR. DART is very different from the existing testing methods. The innovations and main contributions of our paper include the following.

- First, unlike many existing methods, the tree structure of DART is not given but constructed based on the distance matrix via the proposed algorithm 1.
- Second, when testing on this aggregation tree, on higher layers, the nodes and hypotheses are dynamic, *i.e.*, depending on the testing results on the previous layers. Controlling FDR for dynamic hypotheses is challenging. In this paper we introduced new techniques to guarantee the asymptotic validity of DART.

- Third, to make sure DART can be applied to a wide range of application contexts, we relaxed the requirement on the input feature P-values. P-values obtained from asymptotic tests (such as the Wald tests, the score tests, the likelihood ratio tests, *et al*) often slightly deviate from the uniform or sub-uniform distribution though asymptotically they are uniformly or sub-uniformly distributed. For multiple testing problems, the slight deviations could accumulate and eventually inflate FDR. We proposed the new asymptotic oracle P-value definition to guarantee asymptotic FDR control while using some of these P-values.
- Last but not least, we focus on not only the node-level FDR control but also the feature-level FDR control. The feature-level FDR control is more challenging than the node-level FDR control because a node could contain multiple features with mixed null/alternative status. We studied the conditions under which the feature-level can be asymptotically controlled, which sheds light on the appropriate application contexts where DART should be used.

The rest of the paper is organized as follows. Section 2 describes the DART algorithms. Section 3 justifies the asymptotic validity of DART under mild conditions. Section 4 shows that under various models, DART has superior performance than the competing methods. Section 5 applies DART to study the impact hematopoietic stem cell transplantation (HCT) post-transplant care on patient gut microbiota compositions. Section 6 provides a brief discussion on the possible extension of DART. The proofs of propositions and theorems are provided in the appendix. More details on the DART algorithms and the proofs of the lemmas are provided in the supplementary materials.

2 Method

2.1 Model

Denote by $\Omega = \{1, \dots, m\}$ the set with m features. Assume the distance matrix of these features is $D = (d_{ij})_{m \times m}$, where $d_{ij} = d_{ji}$ is the distance between feature i and feature j . It is easy to see that $d_{ii} = 0$. The distance matrix can be scaled so that $\max_{i \neq j} d_{ij} = 1$.

Among these features, let Ω_1 be the important (alternative) feature set, Ω_0 is the unimportant (null) feature set, and $\Omega_1 \cap \Omega_0 = \emptyset$, $\Omega_1 \cup \Omega_0 = \Omega$. For feature i , the hypothesis is

$$H_{0i} : i \in \Omega_0 \quad \text{versus} \quad H_{1i} : i \in \Omega_1. \quad (1)$$

To test $H_{0,i}$, a feature P-value (statistic) T_i is derived.

Definition 1 (Oracle P-value). We call a statistic \tilde{T}_i an oracle P-value if

$$P(\tilde{T}_i \leq p) \leq p \text{ when } i \in \Omega_0 \quad \text{and} \quad P(\tilde{T}_i \leq p) > p \text{ when } i \in \Omega_1.$$

Under many circumstances, the P-values are derived from the asymptotic tests (such as the Wald test, the score test, and the likelihood ratio test), and thus are not oracle P-values; however, they asymptotically converge to the oracle P-values.

Definition 2 (Asymptotic oracle P-value). We call a statistic T_i an asymptotic oracle P-value if

$$\sup_{i \in \Omega_0} \sup_{p \in \mathcal{P}_{i0}} \left| \frac{P(T_i < p)}{P(\tilde{T}_i < p)} - 1 \right| \leq \delta_{0m} \quad \text{with} \quad \lim_{m \rightarrow \infty} \delta_{0m} = o(1), \quad (2)$$

where $\mathcal{P}_{i0} = \left\{ p \in [0, 1] : P(\tilde{T}_i < p) \geq \left\{ m(\log m \log \log m)^{1/2} \right\}^{-1} \right\}$.

In this paper, we assume all the feature P-values are asymptotic oracle P-values. This assumption is easily satisfied by many commonly used models and tests. Here we provide a linear model example with features as outcomes. In fact, we used this model to study the impact of HCT post-transplant care on patient gut microbiota complications. Please see Sec-

tion 5 for details.

Example 1. Consider the linear regression model:

$$\mathbf{Y}_{n \times m} = \mathbf{W}_{n \times p_0} \boldsymbol{\theta}_{p_0 \times m} + \boldsymbol{\epsilon}_{n \times m}, \quad (3)$$

where $\mathbf{Y}_{n \times m} = (\mathbf{Y}_1, \dots, \mathbf{Y}_m)$ is a feature outcome matrix with n observations of m features allowing $m > n$, $\mathbf{W}_{n \times p_0}$ is the design matrix with n observations of p_0 covariants with $p_0 < n$, $\boldsymbol{\epsilon}_{n \times m}$ is the random error matrix with $E(\boldsymbol{\epsilon}) = \mathbf{0}$, and $\boldsymbol{\theta}_{p_0 \times m} = (\boldsymbol{\theta}_1, \dots, \boldsymbol{\theta}_m)$ is the coefficient matrix with $\boldsymbol{\theta}_i \in \mathbb{R}^{p_0}$ the coefficient of \mathbf{W} on \mathbf{Y}_i . In many applications, we would like to test contrasts: for feature i , the hypothesis is $H_{0i} : \mathbf{q}^T \boldsymbol{\theta}_i = 0$. We can use the Wald's test to calculate P-values of $H_{0,i}$. Let $\hat{\boldsymbol{\theta}} = (\hat{\boldsymbol{\theta}}_1, \dots, \hat{\boldsymbol{\theta}}_m)$ be the least square estimator of $\boldsymbol{\theta}$. The Wald's statistic X_i^* and its corresponding P-value T_i is

$$X_i^* = \frac{(\mathbf{q}^T \hat{\boldsymbol{\theta}}_i)^2}{s^2 \mathbf{q}^T (\mathbf{W}^T \mathbf{W})^{-1} \mathbf{q}}, \quad T_i = 1 - F_0(X_i^*), \quad (4)$$

where $s^2 = \frac{1}{n-p_0} \left\| \mathbf{Y}_i - \mathbf{W} \hat{\boldsymbol{\theta}}_i \right\|_2^2$, and F_0 is the CDF of the $\chi^2(1)$ distribution. Here, T_i s are not oracle P-values, but they are asymptotic oracle P-values. Details are provided in Lemma 1 and its proof in the supplementary materials.

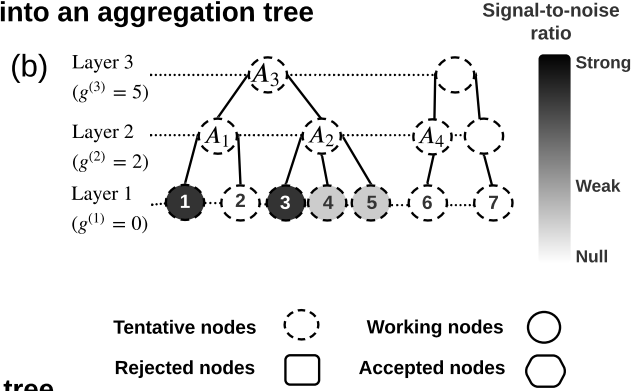
2.2 Two stages of DART

DART has two stages. In stage I, we transform the feature distance matrix into an aggregation tree where closer features are prioritized to be aggregated. In stage II, we embed multiple testing in the constructed aggregation tree and control the feature-level FDR. Utilizing trees to incorporate the distance matrix information can avoid the challenges in estimating the unknown linkage structures between the distance and the hypothesis status, because the hierarchical structure of trees automatically leads to the dynamic exploration of the optimal feature combining levels to adaptively increase the power.

Stage I: Transform the distance matrix into an aggregation tree

(a)

	1	2	3	4	5	6	7
1	0	2	4	5	5	8	11
2	2	0	2	3	3	6	9
3	4	2	0	1	1	8	11
4	5	3	1	0	2	9	12
5	5	3	1	2	0	9	12
6	8	6	8	9	9	0	3
7	11	9	11	12	12	3	0



Stage II: Embed multiple testing in the tree

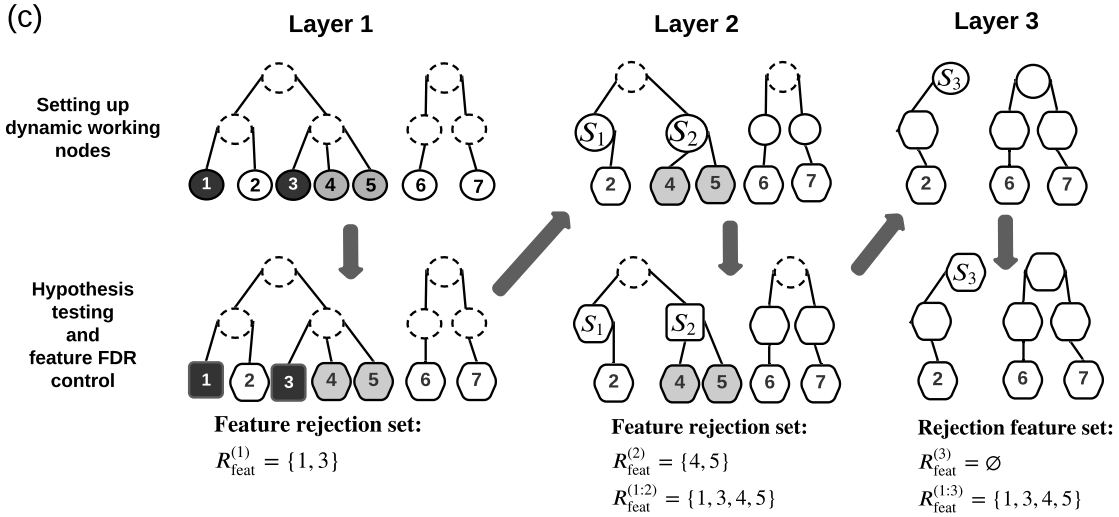


Figure 1: An illustrating example of DART with 7 features. (a) Distance matrix of the 7 features. (b) In stage I, we transfer the distance matrix into the 3-layer aggregation tree based on Algorithm 1. The underlying feature signal-to-noise ratios are illustrated by the gray scales; these ratios are unknown. All nodes at this step are tentative. (c) In stage II, we perform the multiple testing embedded in the aggregation tree. We start from layer 1 and hierarchically proceed to higher layers. When testing on layer ℓ , all previous rejected features are excluded from the temporary nodes (dashed-line circled) to form the working nodes (solid-line circled) on this layer. The rejected nodes are marked by solid squares and the accepted nodes solid hexagons. All the features contained in the rejected nodes are rejected.

2.2.1 Stage I: Transform the distance matrix into an aggregation tree

Before we introduce the tree construction algorithm, we introduce some notations. Denote an L -layer aggregation tree by $\mathcal{T}_L = \{\mathcal{A}^{(\ell)} : \ell = 1, \dots, L\}$, where $\mathcal{A}^{(\ell)}$ is the set of nodes on layer ℓ . Any node $A \in \mathcal{A}^{(\ell)}$ is a set of features. If a node A is aggregated from one or multiple children on layer $\ell - 1$, denote its children set by $\mathcal{C}(A)$. In other words, $A = \cup_{A' \in \mathcal{C}(A)} A'$; and $|\mathcal{C}(A)|$ counts the number of A 's children. For example, in Figure 1b, $A_1 = \{1, 2\}$, $A_2 = \{3, 4, 5\}$, and $\mathcal{C}(A_3) = \{A_1, A_2\}$ with $|\mathcal{C}(A_3)| = 2$. A node could be equal to its child. For example, in Figure 1, $A_4 = \{6\}$ equal to its child. For any two nodes A and B (not necessarily on the same layer), the distance between A and B is $\text{dist}(A, B) = \max_{i \in A, j \in B} d_{ij}$. In Figure 1b, $\text{dist}(A_1, A_2) = 5$. The node distance defined here can be viewed as the complete linkage function initially proposed for hierarchical clusterings (Hastie et al., 2009). Under some special application context, other linkage functions may also be used. For any node A , the diameter of node A is $\text{dia}(A) = \max_{i \in A, j \in A} d_{ij}$. In Figure 1b, $\text{dia}(A_3) = 5$.

In stage I, we would like to construct an aggregation tree based on the feature distance matrix. On layer ℓ ($\ell \geq 2$), we hope that for all $A \in \mathcal{A}^{(\ell)}$

$$\text{dia}(A) \leq g^{(\ell)} \text{ and } |\mathcal{C}(A)| \leq M. \quad (5)$$

The threshold $g^{(\ell)}$ restricts the maximum distance among all features in the node to make sure its containing features are close to each other; thus these features are likely to be co-null or co-alternative. If each of them has weak signal-to-noise ratios, aggregating them will boost their collective signal-to-noise ratio and increase their chance to be discovered. We restrict the nodes' children numbers to reduce the risk of creating mixed nodes (Definition 7) because too many mixed nodes will possibly lead to feature-level FDR inflation (see Section 3). To construct an aggregation tree satisfying 5, we proposed an algorithm based on the Greedy algorithm (Cormen et al., 2001). The pseudo-code of this stage I algorithm is provided in Algorithm 1 in the the supplementary materials (Section S1.1), along with its remarks.

At the end of stage I, an aggregation tree will be derived, with all nodes tentative. In stage II, based on the rejection path, we will further refine those nodes to form working nodes and working hypotheses.

2.2.2 Stage II: Embed multiple testing in the tree

The stage II testing procedure is recursive: On layer ℓ , the working hypotheses, the working P-values, and the P-value threshold depend on all previous layers.

On layer 1, leaf $\{i\}$ is coupled with the original hypothesis $H_{0,i}$ in (1). We reject $H_{0,i}$ if and only if the working P-value $T_i < \hat{t}^{(1)}(\alpha)$, where $\hat{t}^{(1)}(\alpha)$ is a threshold defined as follows.

$$\hat{t}^{(1)}(\alpha) = \left\{ \alpha_m \leq t \leq \alpha : \frac{mt}{\max\{\sum_{i=1}^m I(T_i < t), 1\}} \leq \alpha, \right\} \quad (6)$$

where $\alpha_m = 1/\{m(\log m)^{1/2}\}$. This testing procedure is similar to the Benjamini and Hochberg procedure (Benjamini and Hochberg, 1995) with minor difference at the tail. Similar procedure have been proposed and discussed in other papers such as Liu et al. (2013) and Xie and Li (2018). After the testing procedure on layer 1, denote the rejected feature set by $R_{\text{feat}}^{(1)} = \{i : T_i \leq \hat{t}^{(1)}(\alpha)\}$.

Traditional multiple testing procedure will stop on layer 1. However, DART will continue to aggregate nearby nodes because they are likely to be co-null or co-alternative. If the neighboring nodes all have weak signal-to-noise ratios, after aggregation their aggregated signal-to-noise ratio will be larger, and thus their chance to be discovered will increase..

On layer ℓ ($\ell \geq 2$), suppose the testing on the previous $\ell - 1$ layers yields the rejected feature set $R_{\text{feat}}^{1:(\ell-1)} = \cup_{\ell'=1}^{\ell-1} R_{\text{feat}}^{(\ell')}$, where $R_{\text{feat}}^{(\ell')}$ is the rejected feature set on layer ℓ' . Denote the tentative node set on layer ℓ of the stage I aggregation tree by $\mathcal{A}^{(\ell)}$. For any tentative node $A \in \mathcal{A}^{(\ell)}$, we define $S(A) = A \setminus R_{\text{feat}}^{1:(\ell-1)}$. We call $S(A)$ a *working node*. The rejected features are removed from the working nodes because they have already been rejected and do not need to be tested again. For example, in Figure 1c, layer 1 rejected features 1 and 3; on layer 2,

they are removed from the tentative nodes $A_1 = \{1, 2\}$ and $A_2 = \{3, 4, 5\}$ to form the working nodes $S_1 = \{2\}$ and $S_2 = \{4, 5\}$.

Define the testing node set on layer ℓ :

$$\mathcal{B}^{(\ell)} | \mathcal{Q}^{(1:\ell-1)} = \{S(A) : A \in \mathcal{A}^{(\ell)}, |\mathcal{C}(S(A))| \geq 2\}.$$

Where $\mathcal{C}(S(A)) = \{A' \setminus R_{\text{feat}}^{1:(\ell-1)} : A' \in \mathcal{C}(A)\}$. We exclude the node with only one child because the node must have been tested on some lower layer. For example, in Figure 1c, $S_1 = \{2\}$ has been tested on layer 1. For any $S \in \mathcal{B}^{(\ell)}$, although it is dynamic, given the rejection path $\mathcal{Q}^{(1:\ell-1)}$, they are deterministic. Thus, conditioning on $\mathcal{Q}^{(1:\ell-1)}$, we construct the working node hypotheses:

$$\forall S \in \mathcal{B}^{(\ell)}, \quad H_{0S} : \forall j \in S, j \in \Omega_0 \quad \text{versus} \quad H_{1S} : \exists j \in S, j \in \Omega_1,$$

On layer ℓ , we aim to develop a multiple testing approach to simultaneously test these (conditional) working node hypotheses while asymptotically controls the feature-level FDR.

Definition 3 (Node working P-values). For any node A , suppose T_j with $j \in A$ are the feature P-values. Then the node's working P-value is defined as

$$X_j = \bar{\Phi}^{-1}(T_j), \quad X_A = \sum_{j \in A} X_j / \sqrt{|A|}, \quad T_A = \bar{\Phi}(X_A), \quad (7)$$

where $\bar{\Phi}$ is the complementary CDF of the standard Gaussian distribution.

Noteworthy, working P-values are not oracle P-values. Because S is dynamic, the distribution of T_S depends on $\mathcal{Q}^{(1:\ell-1)}$. In Lemma 2 and 3, we will show T_S still has a good approximation to oracle p-value:

$$\sup_{S \in \mathcal{B}_0^{(\ell)}} \sup_{p \geq 1/m} \mathbb{P}(T_S \leq p | \mathcal{Q}^{(1:\ell-1)}) \leq p(1 + o(1)).$$

Similar to other multiple testing procedures, we threshold the working P-values to reject the

nodes. For all $S \in \mathcal{B}^{(\ell)}$, H_{0S} is rejected if $T_S < \hat{t}^{(\ell)}(\alpha)$, where

$$\hat{t}^{(\ell)}(\alpha) = \sup \left\{ \alpha_m \leq t \leq \alpha : \frac{\sum_{\ell'=1}^{\ell-1} m^{(\ell')} \hat{t}^{(\ell')}(\alpha) + m^{(\ell)} t}{\max\{|R_{\text{feat}}^{(1:\ell-1)}| + \sum_{S \in \mathcal{B}^{(\ell)}} |S| I(T_S < t), 1\}} \leq \alpha \right\}, \quad (8)$$

Here $\alpha_m = 1/\{m(\log m)^{1/2}\}$ and $m^{(\ell)} = \sum_{S \in \mathcal{B}^{(\ell)}} |S|$. For simplicity sake, we use $\hat{t}^{(\ell)}$ to present $\hat{t}^{(\ell)}(\alpha)$ in the rest of the paper. It is easy to see that $\hat{t}^{(\ell)}$ is recursive.

After applying the rejection rule (8), let

$$\mathcal{R}_{\text{node}}^{(\ell)} = \{S \in \mathcal{B}^{(\ell)} : T_S < \hat{t}^{(\ell)}\}, \quad R_{\text{feat}}^{(\ell)} = \cup_{S \in \mathcal{R}_{\text{node}}^{(\ell)}} S.$$

If a working node is rejected, We reject all its features. Although this rejection rule is aggressive, it is reasonable when most close features have co-null/co-alternative patterns. In Section 3, we will show this rule asymptotically controls feature-level FDR under mild conditions. The pseudo-code of the stage II algorithm is provided in Algorithm 2 in the supplementary materials (Section S1.2).

2.3 Tuning parameter selection

The number of total layers L , the maximum cardinality M , and the distance upper bounds $g^{(2)}, \dots, g^{(L)}$ are viewed as tuning parameters. Here we provide a feasible approach to select the tuning parameters.

- $M = 3$. If M is too large, nodes on the aggregation tree are more likely to be mixed nodes (Definition 7) and the FDR will likely to be inflated. If M is too small, when weak signal-to-noise ratio features aggregate, their collective signal-to-noise ratios might still be too small to be identified. Numerical studies show that $M = 3$ performs well in practice.
- $L = \lceil \log_M m - \log_M c_m \rceil$, where c_m is the desired minimal number of working nodes on layer L . This is because on layer L , c_m will be lower bounded by m/M^L .
- The distance thresholds $g^{(1)}, \dots, g^{(L)}$ are set recursively based on the criterion of max-

imizing the number of testable nodes on each layer. Let $g^{(1)} = 0$ and $G = \{g_1, \dots, g_K\}$ be the candidate threshold set. On layer ℓ , let $G^{(\ell)} = \{g \in G : g > g^{(\ell-1)}\}$. For any $g \in G^{(\ell)}$, let $\mathcal{A}^{(\ell)}(g)$ be the resulting node set based on Algorithm 1. Then we set $g^{(\ell)}$ as

$$g^{(\ell)} = \arg \max_{g \in G^{(\ell)}} |\tilde{\mathcal{A}}^{(\ell)}(g)|, \quad \text{where } \tilde{\mathcal{A}}^{(\ell)}(g) = \{A : A \in \mathcal{A}^{(\ell)}(g), |\mathcal{C}(A)| \geq 2\}.$$

3 Asymptotic Theory

In this section, we first introduce conditions and theorems to asymptotically control the weighted node-level FDR. Then we discuss how to asymptotically control feature-level FDR. The latter is more challenging.

The common challenges for both parts stem from the dynamic properties in nodes and node hypotheses, *i.e.*, when testing on layer ℓ , the nodes and the testing procedure depend on the testing results on the previous layers. Meanwhile, the conditions only describe the properties of the static features or nodes constructed from stage I. We developed new techniques to fill in the gap. Specifically, we carefully analyzed the relationship between the feature signal strength level and its rejection probability on each layer. By this way, we can predict the rejection path of some features probabilistically and based on them to develop the theorems to asymptotically control the FDRs.

3.1 Weighted node-level FDR control

In multiple testing, type I error is commonly measured by the false discovery proportion (FDP) and its expectation, the false discovery rate (FDR). Under our model, we defined the weighted node-level FDP and FDR up to layer ℓ as

$$\text{FDP}_{\text{node}}^{(1:\ell)} = \frac{\sum_{\ell'=1}^{\ell} \sum_{S \in \mathcal{R}_{\text{node}}^{(\ell')} \cap \mathcal{B}_0^{(\ell')}} |S|}{\{\sum_{\ell'=1}^{\ell} \sum_{S \in \mathcal{R}_{\text{node}}^{(\ell')}} |S|\} \vee 1}. \quad \text{FDR}_{\text{node}}^{(1:\ell)} = E(\text{FDP}_{\text{node}}^{(1:\ell)}),$$

Clearly, the denominator of $\text{FDP}_{\text{node}}^{(1:\ell)}$ counts the weighted number of all rejected nodes (taking maximum with 1 to avoid the denominator being 0), and numerator counts the weighted number of falsely rejected nodes; each node is weighted by its cardinality. Thus, a larger falsely rejected node will inflate the weighted node-level FDR more than a smaller falsely rejected node. We use the weight node-level FDP and FDR here because it can be more easily connected with the feature-level FDP and FDR. See Section 3.2.

To control the weighted node-level FDR, we introduce the following conditions.

Condition 1. Assume $m_1 \leq r_2 m^{r_1} \leq r_2 n^{r_1/r_3}$ for some $r_1 < (M^{L-1} + 1)^{-1}$, $r_2 > 0$, and $r_3 > 0$.

Condition 1 assumes the important features are sparse, and the number of features is bounded by certain polynomial order of the sample size, $n \geq m^{r_3}$.

For any node A , we define its descendant set as

$$\mathcal{D}(A) = \{D : \exists \ell, \text{ such that } D \in \mathcal{A}^{(\ell)} \text{ and } D \subsetneq A\}.$$

For example, in Figure 1b, $\mathcal{D}(A_3) = \{A_1, A_2, \{1\}, \{2\}, \{3\}, \{4\}, \{5\}\}$.

Definition 4 (Moderately strong Signal-to-Noise Ratio (SNR) nodes). A node A is called a moderately strong SNR node if

$$\text{P}\{T_A < \alpha_m, \forall D \in \mathcal{D}(A), T_D \geq \bar{\Phi}(m^{r_1-1} \sqrt{\log m})\} \geq C_1 > 0, \quad (9)$$

where α_m is the P-value thresholds lower bound defined in (8).

In fact, (9) is related to the alternative feature SNR. To better illustrate the moderately strong SNR nodes, we provide an equivalent definition when the test statistics follow the Normal distribution.

Example 2 (Normal distribution example). Suppose for feature i , a test statistic $Z_i \sim \text{N}(\tau_i, 1)$ can be derived. The hypotheses are

$$H_{0i} : \tau_i = 0 \quad \text{versus} \quad H_{1i} : \tau_i \neq 0.$$

The P-values are $T_i = 2\bar{\Phi}(|Z_i|)$.

Under Example 2, a node A satisfying equation (9) when

$$\forall i \in A, \quad |\tau_i| \in [\gamma_m/\sqrt{|A|}, \beta_m/\sqrt{|A|-1}].$$

where

$$\beta_m = \sqrt{2(1-r_1)\log m - 2\log\log m}, \quad \gamma_m = \sqrt{2\log m + \log\log m}. \quad (10)$$

Although both β_m and γ_m increase with m , the rate is slow. In practice, when the sample size n increases, τ_i will increase with n , often at the rate of \sqrt{n} . Compared with \sqrt{n} , both β_m and γ_m are relatively small.

For any moderately strong SNR node A , suppose $A \in \mathcal{A}^{(\ell)}$. We will prove that with a certain non-vanishing probability, none of A 's descendants will be rejected on the previous layers but A will be rejected on layer ℓ . On the tree \mathcal{T}_L , denote the set of all moderately strong SNR nodes by \mathcal{A}_{md} . Define $c_{\text{md}} = \min_{\ell \in \{1, \dots, L\}} |\mathcal{A}_{\text{md}} \cap \mathcal{A}^{(\ell)}|$ as the minimal number of moderately strong SNR nodes across all layers.

Condition 2. For some constant $r_4 > 0$, $c_{\text{md}} \geq r_4 \log m$.

A node on layer ℓ has at most $M^{\ell-1}$ features, thus level ℓ has at least $M^{-\ell+1}m_1$ alternative nodes. Because we allow $m_1 = O(m^{r_1})$ by Condition 1, the total number of the alternative nodes (containing alternative features) is also allowed to reach $O(m^{r_1})$. Condition 2 only requires $c_{\text{md}} \geq r_4 \log m$ among them are moderately strong SNR node; therefore, this condition is very weak.

For any node A on the top layer of \mathcal{T}_L , define its dependent node set as

$$\Gamma_A = \{A' \in \mathcal{A}^{(L)} : \{T_i, i \in A \cup A'\} \text{ are dependent}\}. \quad (11)$$

We assume Γ_A is relatively small for most of the As . We allow the existence of a) self-dependent nodes whose features are dependent and b) hub nodes which are dependent with many other nodes, but these nodes cannot be too many.

Condition 3 (Few self-dependent and hub nodes). Define $\mathcal{A}' = \{A \in \mathcal{A}^{(L)} : |\Gamma_A| \geq \delta_{2m} = o(\sqrt{c_{\text{md}}})\}$. Assume $|\mathcal{A}'| = o(c_{\text{md}})$.

Under these conditions, the weighted node-level FDP of DART will be under control and thus also for the weighted node-level FDR.

Theorem 1 (Weighted node-level FDP and FDR control). *Under Conditions 1-3, at any pre-specified level $\alpha \in (0, 1)$, DART satisfies the following two statements.*

(1) For any $\epsilon > 0$, $\lim_{m,n \rightarrow \infty} \mathbb{P}(\text{FDP}_{\text{node}}^{(1:\ell)} \leq \alpha + \epsilon) = 1$. Consequently, $\lim_{m,n \rightarrow \infty} \text{FDR}_{\text{node}}^{(1:\ell)} \leq \alpha$.

(2) Let $\tilde{\Omega}_0 = \{j : \tilde{T}_j \text{ follows Unif}(0, 1)\}$, where \tilde{T}_j is the oracle P-value of feature j . If

$$\lim_{m \rightarrow \infty} |\tilde{\Omega}_0|/m = 1, \quad (12)$$

then for all $\epsilon > 0$,

$$\lim_{m,n \rightarrow \infty} \mathbb{P}(|\text{FDP}_{\text{node}}^{(1:\ell)} - \alpha| \leq \epsilon) = 1, \quad \lim_{m,n \rightarrow \infty} \text{FDR}_{\text{node}}^{(1:\ell)} = \alpha.$$

3.2 Feature-level FDR control

Define the feature-level FDP and FDR up to layer ℓ as

$$\text{FDP}_{\text{feat}}^{(1:\ell)} = \frac{|R_{\text{feat}}^{(1:\ell)} \cap \Omega_0|}{|R_{\text{feat}}^{(1:\ell)}| \vee 1}, \quad \text{FDR}_{\text{feat}}^{(1:\ell)} = E(\text{FDP}_{\text{feat}}^{(1:\ell)}).$$

It is easy to see that

$$\begin{aligned} \sum_{\ell'=1}^{\ell} \sum_{S \in \mathcal{R}_{\text{node}}^{(\ell')}} |S| &= \left| \bigcup_{\ell'=1}^{\ell} \bigcup_{S \in \mathcal{R}_{\text{node}}^{(\ell')}} S \right| = |R_{\text{feat}}^{(1:\ell)}| \\ \sum_{\ell'=1}^{\ell} \sum_{S \in \mathcal{R}_{\text{node}}^{(\ell')} \cap \mathcal{B}_0^{(\ell')}} |S| &= \left| \bigcup_{\ell'=1}^{\ell} \bigcup_{S \in \mathcal{R}_{\text{node}}^{(\ell')} \cap \mathcal{B}_0^{(\ell')}} S \right| \leq |R_{\text{feat}}^{(1:\ell)} \cap \Omega_0|. \end{aligned}$$

Thus $\text{FDP}_{\text{node}}^{(1:\ell)} \leq \text{FDP}_{\text{feat}}^{(1:\ell)}$. Controlling $\text{FDR}_{\text{node}}^{(1:\ell)}$ is easier than controlling $\text{FDR}_{\text{feat}}^{(1:\ell)}$. The challenge in controlling $\text{FDR}_{\text{feat}}^{(1:\ell)}$ lies in the existence of those nodes containing both null and alter-

native features. If such nodes are rejected, they are counted as true rejections for node-level weighted FDR control, but the null features in these nodes are counted as false rejections for feature-level FDR control.

Before we formally define those challenging nodes, we first define the strong SNR feature set $\Omega_{\text{st}}^{(1:L)}$ and the weak SNR feature set Ω_{wk} .

Definition 5 (Strong SNR feature set). Let $\Omega_{\text{st}}^{(1:0)} = \emptyset$. On layer ℓ , recursively define

$$\mathcal{A}^{*,(\ell)} = \{A \setminus \Omega_{\text{st}}^{(1:\ell-1)} : A \in \mathcal{A}^{(\ell)}\},$$

and the strong SNR node set as

$$\mathcal{G}_{\text{st}}^{(\ell)} = \{S \in \mathcal{A}^{*,(\ell)} : \forall j \in S, \mathbb{P}\{T_j \in \kappa(|S|)\} > 1 - o(m^{-r_1})\}, \quad (13)$$

where $\kappa(S) = [m^{-\frac{1-r_1}{|S|-1}}, \{m(\log m \log \log m)^{1/2}\}^{-1/|S|}]$. Then the strong SNR feature set on layer ℓ and up to layer ℓ are

$$\Omega_{\text{st}}^{(\ell)} = \cup_{S \in \mathcal{G}_{\text{st}}^{(\ell)}} S, \quad \Omega_{\text{st}}^{(1:\ell)} = \cup_{\ell'=1}^{\ell} \Omega_{\text{st}}^{(\ell')}.$$

Under Example 2, $\mathbb{P}\{T_j \in \kappa(|S|)\} > 1 - o(m^{-r_1})$ in (13) is satisfied when

$$|\tau_j| \in \left(\frac{\gamma_m}{\sqrt{|S|}} + \lambda_m, \frac{\beta_m}{\sqrt{|S|-1}} - \lambda_m \right),$$

where $\lambda_m = \sqrt{2r_1 \log m}$.

We will prove that with a high probability converging to 1, none of the features in $\cup_{S \in \mathcal{G}_{\text{st}}^{(\ell)}} S$ will be rejected from layer 1 to layer $\ell - 1$ but all of them will be rejected on layer ℓ .

Definition 6 (Weak SNR feature set). Let $\iota = (0, m^{\frac{r_1-1}{M^{L-1}}})$. Define the weak SNR feature set

$$\Omega_{\text{wk}} = \{j \in \Omega_1 : \mathbb{P}(T_j \in \iota) = o(m^{-r_1})\}. \quad (14)$$

Under Example 2, $\mathbb{P}(T_j \in \iota) = o(m^{-r_1})$ in (14) is satisfied when

$$|\tau_j| \in (0, \beta_m / \sqrt{M^{L-1}}).$$

When a node S contains only null features and weak signal features, then the probability of rejecting S is negligible.

Definition 7 (mixed nodes). For any node $A \in \mathcal{A}^{(\ell)}$, let

$$A^* = A \setminus (\Omega_{\text{st}}^{(1:\ell-1)} \cup \Omega_{\text{wk}}), \quad A_0^* = A^* \cap \Omega_0, \quad A_1^* = A^* \cap \Omega_1. \quad (15)$$

If $A_0^* \neq \emptyset$ and $A_1^* \neq \emptyset$, we call A a mixed node.

Noteworthy, not all nodes containing both null and alternative features are called mixed nodes. For example, suppose node $A \in \mathcal{A}^{(\ell)}$ have three child nodes $\mathcal{C}(A) = \{A_1, A_2, A_3\}$, where $A_1 \subset \Omega_{\text{st}}^{(\ell-1)}$, $A_2 \subset \Omega_{\text{wk}}$, and A_3 contains all null features. Although both null and alternative features exist in node A , this is not a mixed node. This is because A_1 will be rejected on layer $\ell - 1$ with high probability converging to 1 so that A 's corresponding working node S is probably $A_2 \cup A_3$; also, S will not be rejected on layer ℓ with probability converging to 1 so that FDR will not be inflated. Define the strong and weak feature set will further narrow down the mixed nodes so that the condition to restrict their number (Condition 4) becomes weaker.

Condition 4 (Sparse mixed nodes). Let $\mathcal{P} = \{S \in \mathcal{A}^{(L)} : S \text{ is a mixed node}\}$. Then $|\mathcal{P}| = o(c_{\text{md}})$.

Condition 4 assumes that the mixed nodes on layer L (the top layer) are rare. Equivalently, this means the dominating majority of the nodes contain: 1) only null features; 2) only alternative features; 3) a combination of null and alternative features but all alternative features are either weak or strong SNR features. Because the aggregation tree is constructed based on the distance matrix, this condition can be translated as how distance informs hypothesis states (null or alternative). To prove the consistence of the overall FDP, we need this condition because our rejection rule aggressively rejects all features in a node if the node is rejected. Without Condition 4 we might reject too many mixed nodes so that the feature-level FDR could be inflated.

Theorem 2 (Overall feature FDR control). *Under Conditions 1-4, at any pre-specified level $\alpha \in (0, 1)$, DART satisfies the following two statements.*

(1) *For any $\epsilon > 0$, $\lim_{m,n \rightarrow \infty} \mathbb{P}(\text{FDP}_{\text{feat}}^{(1:\ell)} \leq \alpha + \epsilon) = 1$. Consequently, $\lim_{m,n \rightarrow \infty} \text{FDR}_{\text{feat}}^{(1:\ell)} \leq \alpha$.*

(2) *If (12) holds, then for any $\epsilon > 0$,*

$$\lim_{m,n \rightarrow \infty} \mathbb{P}(|\text{FDP}_{\text{feat}}^{(1:\ell)} - \alpha| \leq \epsilon) = 1, \quad \lim_{m,n \rightarrow \infty} \text{FDR}_{\text{feat}}^{(1:\ell)} = \alpha.$$

4 Numerical results

In this section, the simulation results are carried out to evaluate the performance of DART. We simulate m features located in the two-dimensional Euclidean space with randomly generated location coordinates: the first coordinate follows $\text{N}(0, 2)$, and the second coordinate follows $\text{Unif}(0, 4)$. A distance matrix $\mathbf{D} = (d_{i,j})_{m \times m}$ is calculated based on the feature location coordinates. Two different feature settings are considered, $m = 100$ and $m = 1000$. When $m = 100$, we generate $m_1 = 22$ alternative, and $n = 90$ samples. When $m = 1000$, we generate $m_1 = 141$ alternatives, and $n = 300$ samples.

Based on the tuning parameter selection criterion in Section 2.3, we construct a 2-layer aggregation tree when $m = 100$ and a 4-layers aggregation tree when $m = 1000$. More details about the tuning parameters settings and their selection procedure are shown in supplementary materials 2.3.

We consider five different model settings, SE1–SE5.

Throughout the five settings, the hypotheses are:

$$H_{0,i} : \theta_i = 0 \quad \text{against} \quad H_{1,i} : \theta_i \neq 0, \quad i \in \Omega.$$

SE1 simulates the working P-values satisfying the oracle P-value property, and thus mimics the ideal situation. SE2 and SE3 simulates the working P-values by mis-specifying the null distributions, and thus these P-values do not satisfy the oracle P-value property. We use these

two settings to evaluate the robustness of DART and the competing methods. SE4 simulates the linear regression model and SE5 simulates the Cox proportional hazard model. The feature P-values are derived from the Wald tests. We are interested to see how DART compares to the competing methods under these two commonly used models. Details in how to generate these simulation settings are displayed in the supplementary materials (Section S2.1). Under each setting, the simulation is repeated 200 times. The R codes are available at https://github.com/xxli8080/DART_Code.

We set the nominal FDR at the level $\alpha = 0.05, 0.1, 0.15, 0.20$. We followed Section 2.3 to select the tuning parameters; details are displayed in the supplementary materials (Section S2.2). DART successfully controlled the empirical FDR under the desired level. The FDR control is robust when the model is misspecified. Figure 2 shows how DART performs when the algorithm stopped at different layers. Obviously, the one-layer DART is the same as the traditional single layer multiple testing method which ignores the distance matrix. As the number of maximum layers L goes up, more alternative features are aggregated and identified. Notably, increasing the nominal FDR level cannot lead to such great increase in sensitivity.

We also compared the performance of DART with the two FDR_L procedures (FDR_L I and FDR_L II) proposed by Zhang et al. (2011). The two procedure adjust each feature's P-value according to its k -nearest neighbors; the adjusted p-value is the median of its neighborhood p-values. The FDR_L I and FDR_L II procedures use different methods to estimate the distribution of the adjusted P-values. We compared to both procedures in our simulation. To perform a fair comparison, we also tried a wide range of choices $k \in \{2, 3, \dots, 9\}$. When $(n, m) = (90, 100)$, both FDR_L I and FDR_L II led to FDR inflation regardless of the choice of k . When $(n, m) = (300, 1000)$, the FDR_L I procedure constantly led to inflated FDR, while the FDR_L II procedure led to the desired FDR when $k \leq 7$ but the sensitivity is lower than DART. Figure 2 presents the performance of FDR_L procedures with $k = 2, 3$ when $(n, m) = (90, 100)$ and $k = 6, 7$ when $(n, m) = (300, 1000)$, because under these k settings, the FDR_L procedures perform the best. One reason that the FDR_L procedures did not perform as well as DART is that the methods

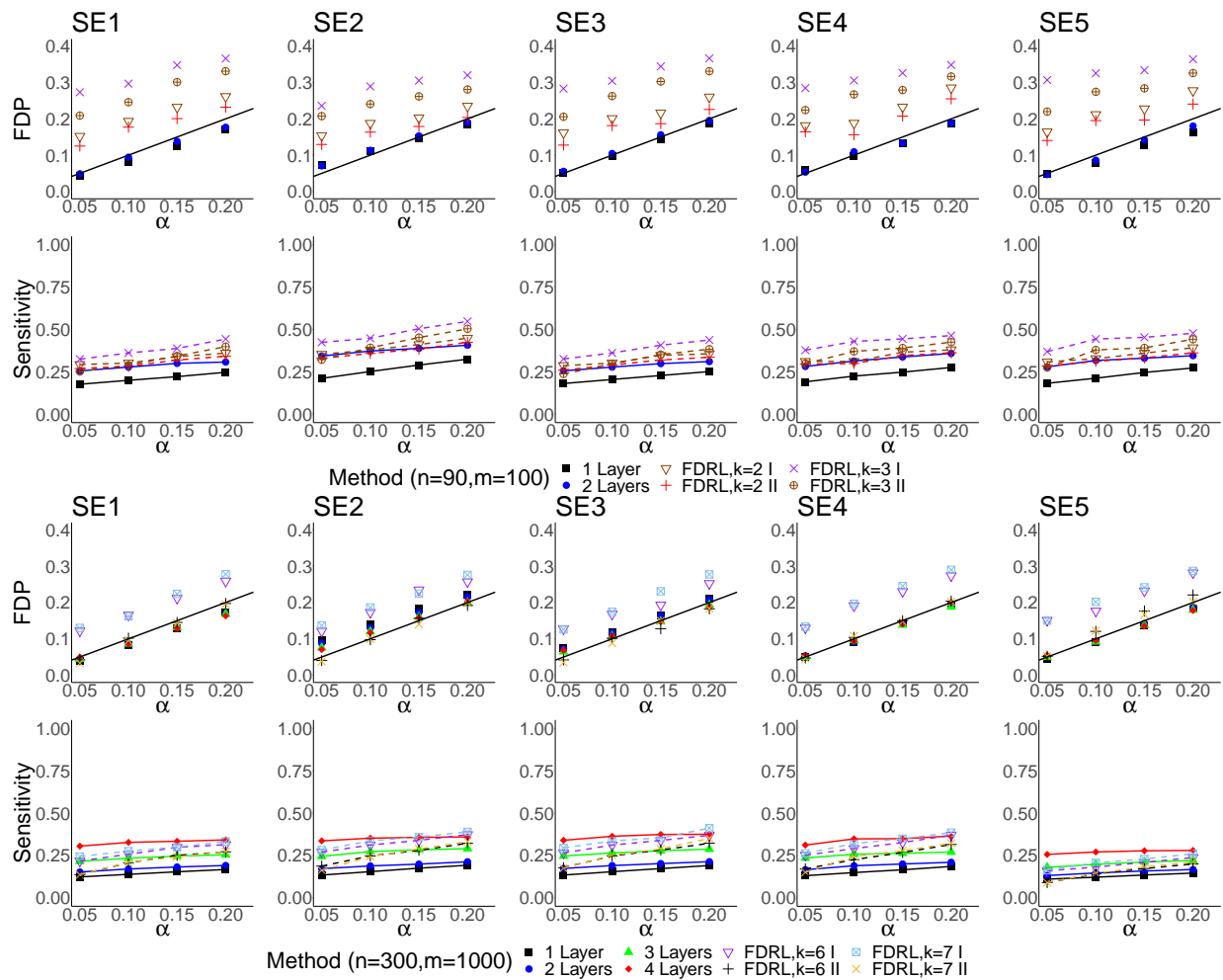


Figure 2: Simulation results for setting SE1-SE5. The first two rows represent the results in the setting $(n, m) = (90, 100)$, and the second two rows represent the results in the setting $(n, m) = (300, 1000)$.

use a constant k to aggregate P-values. Very often, the distance among features often cannot be fully captured by the neighborhood with constant number of neighbors. For example, an feature far away from all other features also have k nearest neighbors; however, the isolated feature and its neighbors often do not share co-importance. Thus, FDR_L does not perform well under these settings.

5 Data Analysis

We apply DART to a clinical trial on the hematopoietic stem cell transplantation (HCT), where microbiome data are collected from 144 leukemia patients before and after the HCT. Graft-versus-host disease (GVHD) is one of the major complications of the HCT. Recent studies have linked GVHD to the disruptions of the gut microbiome (Jenq et al., 2012), and the disruptions may be related to the environmental changes such as post-transplant care (Claesson et al., 2012). The goal of this study is to investigate the potential impact of the post-transplant care (home care versus standard hospital care) on the patient gut microbiota composition.

To achieve the goal, the patient fecal samples are collected before and after HCT; the fecal microbiome are sequenced by the 16S ribosomal RNA sequencing at the Memorial Sloan Kettering Cancer Center. The data are then pre-processed by the R package, DADA2 (Callahan et al., 2016), to generate the amplicon sequence variants (ASV) and the read counts. Samples with less than 200 total read counts and the ASVs with read counts fewer than 4 in more than 80% of the samples are removed from the analysis. After the pre-processing procedure, the data set contains 288 samples (before- and after- HCT) from 144 patients, each with 97 ASVs. The data are available at https://github.com/xxli8080/DART_Code/tree/master/Data_Analysis. In our analysis, to increase computation stability, the zero counts are replaced by 0.5 (Aitchison, 1982; Kurtz et al., 2015).

In microbiome studies, the ASV abundance compositions are more meaningful than the absolute read counts. To modeling the compositional microbiome data, we use the additive log-ratio

transformation proposed by Aitchison (1982). Specifically, we choose the most abundant ASV (the ASV with the largest median read counts across all patients) as the reference ASV, and define M_i as the log read counts ratio between the ASV i and the reference ASV. For example, for a patient, if the read counts of ASV i and the reference ASV are 100 and 200 respectively, then $M_i = \log(100/200) = -\log 2$.

Because one ASV is chosen as the reference ASV, the distance matrix is calculated among the remaining 96 non-reference ASV using the R package `Phangorn` (Schliep, 2011) based on the JC69 model (Jukes et al., 1969). The JC69 model is a classical Markov model of DNA sequence evolution and can be used to estimate the evolutionary distance between sequences. Two ASVs with similar sequences tend to be close with each other, and more likely to perform similar biological functions. Therefore, we will incorporate the distance matrix in identifying the important ASVs. We use the linear model, defined in (3) with $p_0 = 3$, to regress the microbiome composition changes before and after HCT on the after-transplantation care (home care vs. hospital care) and other covariates. Specifically, for the non-reference ASV i , $i \in \{1, \dots, 96\}$,

$$M_{1,i} - M_{0,i} = \theta_{1,i}W_1 + \theta_{2,i}W_2 + \theta_{3,i}W_3 + \epsilon_i \quad (16)$$

Here, $M_{0,i}$ (and $M_{1,i}$) is the log counts ratio between ASV i and the reference ASV before (and after) the transplant. Thus $M_{1,i} - M_{0,i}$ is the corresponding Y_i in the model (3). In addition, $W_1 = 1$ is the intercept term, W_2 is the type of care, W_3 is the length of the care (the gap between the HCT surgery and the after-care sample collection), and the $\epsilon \sim N(0, \sigma^2)$ is the random error term with unknown σ^2 . To check whether the after-transplant care affects the ASV compositions, we set up the hypotheses $H_{0i} : \theta_{2,i} = 0$, $i = 1, \dots, 96$. The P-value T_i are calculated based on the Wald tests.

Based on the tuning parameter selection procedure described in Section 2.3, we construct an aggregation tree with $M = 3$, $L = \lceil \log_M 96 - \log_M 30 \rceil = 2$, and $g^{(2)} = 8/\sqrt{144 \log 96 \log \log 96}$. The aggregation tree has 33 non-single-child nodes on the second layer. The nominal FDR level is set at 0.1.

The performance of the DART is compared with two competing methods: 1) BH procedure; 2) FDR_L . For the FDR_L I and II procedures, we considered $k = 2$ or 3. Figure 3(a) shows that the ASVs that are close to each other tend to have similar (small or large) P-values. This suggests that the co-importance pattern among similar ASVs might hold here. In the end, the two-layer DART identified 9 important ASVs while the traditional BH procedure did not identify any ASV. Both FDR_L I and FDR_L II procedures identified 14 important ASVs when $k = 2$. When $k = 3$, FDR_L I identified 16 important ASVs, and FDR_L II identified 7 important ASVs.

In order to evaluate the stability of these methods, we conduct the bootstrap with 200 resamplings. For a specific testing method, the rejection rate of an ASV is calculated as the ratio of the times that the ASV is identified in the 200 rounds of resamplings. If a method is stable, an ASV should tend to be consistently rejected or accepted. In other words, for a valid and powerful test, most null ASVs are expected to have small rejection rates, and very few alternative ASVs are expected to have high rejection rates. Figure 3(b) shows that DART and BH procedures generates the histograms with a peak rejection rate within $[0, 0.2)$, while FDR_L have the peak rejection rate between $[0.1, 0.3)$. Table 1 listed the proportion of ASVs with large (> 0.8) or small (≤ 0.1) rejection rates for each method. Compared with FDR_L method, DART and BH have a higher proportion of ASVs with small rejection rates, indicating both DART and BH have lower risk in FDR inflation. Meanwhile, FDR_L methods have a small proportions of ASVs with the rejection rate within $0 - 0.1$, indicating it is not stable in accepting null ASVs. On the other hand, DART also has a higher proportion of ASVs with large rejection rates comparing to the BH method. This indicates that DART has a robust high power.

Table 1: Summary of the bootstrap results. (RR stands for rejection rates)

Method	RR ≤ 0.1	RR > 0.8
DART	0.27	0.02
BH	0.47	0
FDR_L I, $k = 2$	0.01	0.03
FDR_L I, $k = 3$	0	0.04
FDR_L II, $k = 2$	0.09	0.02
FDR_L II, $k = 3$	0.1	0.03

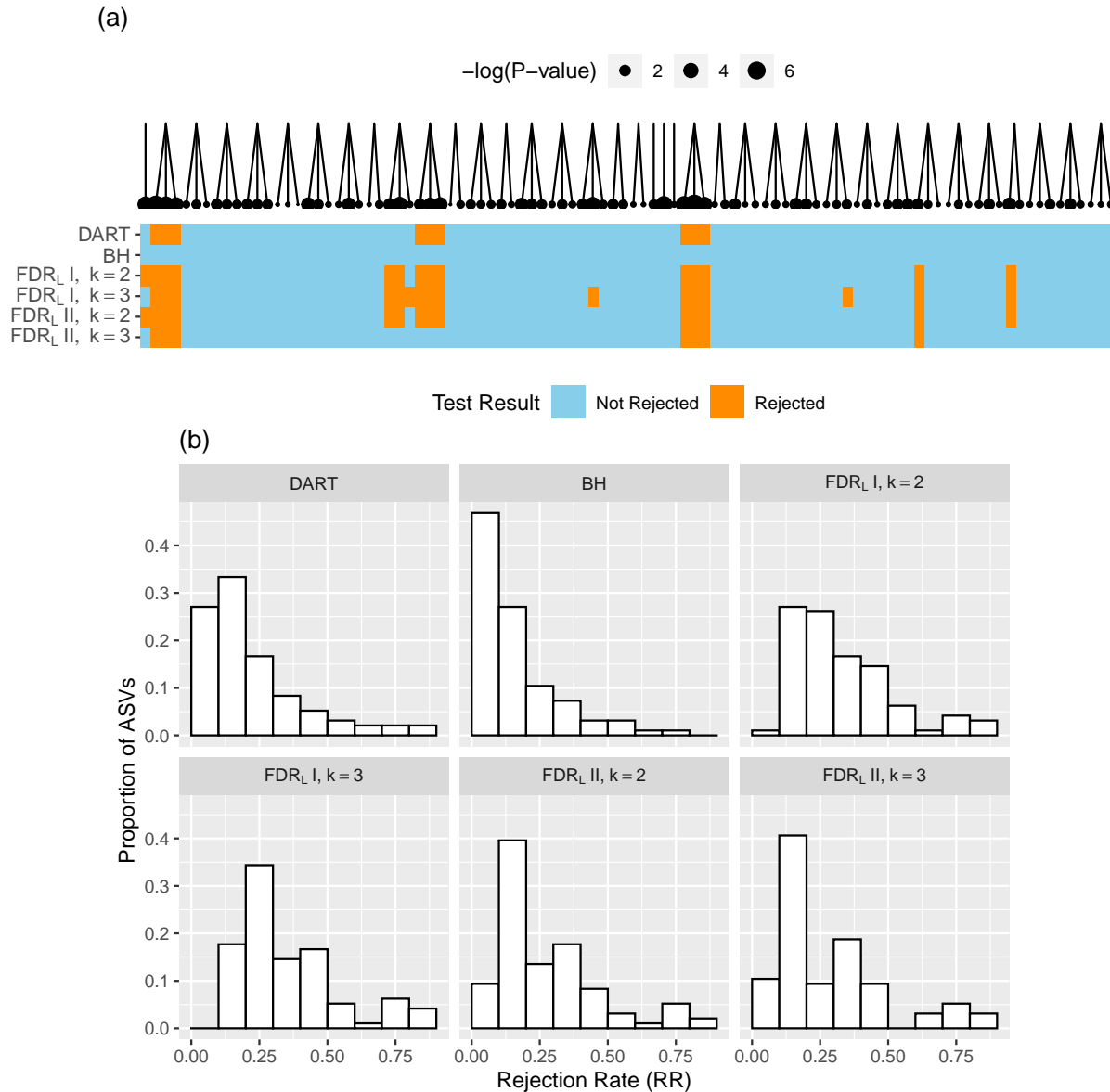


Figure 3: (a) Illustration of the leaf P-values, the aggregation tree, and the testing results. The leaf size is scaled according to the inverse of the P-values. The testing results of different methods are shown in different rows, with blue blocks representing the accepted non-reference ASVs and orange blocks representing the rejected non-reference ASVs. (b) Histograms of ASV rejection rate across the bootstrap with 200 re-samplings.

6 Discussion

In this paper, we developed a novel multiple testing method, DART, to incorporate feature distance in multiple testing. Under many application contexts, the feature distances serve as auxiliary information of their co-importance pattern. DART utilizes this information to boost the testing power. DART applies to the P-values obtained from many asymptotic tests, and thus can work with a wide range of models.

Stage 1 of DART involves constructing an aggregation tree. We provided Algorithm 1 to construct the aggregation tree. Other algorithms may also work, and result in a different aggregation tree from the same distance matrix. Consequently, Stage 2 testing process could lead to different results based on different trees. In practice, if several aggregation trees exist, DART can be applied to all of them, and we can take the one with the most rejections. The asymptotic validity will still hold for this procedure.

DART is a multiple testing method embedded in a hierarchical tree that constructed from the distance matrix. It can be easily extended to the case where other information implies the co-importance pattern of the features. Such information could from domain knowledge, external data sets, or other resources. In addition, the hierarchical testing ideas and techniques can also be extended to solve other multiple testing problems.

Appendix: Proof of the Main Theorems

Before the proof, we need to introduce some further notations. On layer ℓ , for a working node $S \in \mathcal{B}^{(\ell)}$, let $\mathcal{U}(S) = \{S' \subset S : S' \in \cup_{\ell'=1}^{\ell-1} \mathcal{B}^{(\ell')}\}$ be the collection of sets in the testing path of S . In addition, let $\mathcal{U}^c(S) = \{S'' \in \cup_{\ell'=1}^{\ell-1} \mathcal{B}^{(\ell')} : S'' \cap S = \emptyset, S'' \cup S \subset A, \text{ for some } A \in \mathcal{A}^{(\ell)}\}$ be the collection of sets that was planning to combined with S on layer ℓ of the static aggregation tree but rejected on previous layers. When $S \in \mathcal{B}^{(1)}$, we set $\mathcal{U}(S) = \mathcal{U}^c(S) = \emptyset$. We define $G_S(c)$ as the complementary CDF conditional on previous testing results. When $\ell = 1$, we

have $S = \{i\} \subset \{1, \dots, m\}$, and $G_S(c) = P(Z_i \geq c)$ with $Z_1, \dots, Z_m \stackrel{iid}{\sim} N(0, 1)$. When $\ell > 1$, the oracle rejection path for set $S \in \mathcal{B}^{(\ell)}$ is recursively defined as

$$\mathcal{Q}_z^{(1:\ell-1)} = \{z : \forall S' \in \mathcal{U}(S), G_{S'}(Z_{S'}) \geq \hat{t}^{(\ell_{S'})}(\alpha), \forall S'' \in \mathcal{U}^c(S), G_{S''}(Z_{S''}) \leq \hat{t}^{(\ell_{S''})}(\alpha)\},$$

where

$$G_S(c) = P(Z_S \geq c | \mathcal{Q}_z^{(1:\ell-1)})$$

and $Z_S = \sum_{i \in S} Z_i / \sqrt{|S|}$, and $\ell_{S'}, \ell_{S''} \in \{1, \dots, \ell - 1\}$ is the value s.t. $S' \in \mathcal{B}^{(\ell_{S'})}$ and $S'' \in \mathcal{B}^{(\ell_{S''})}$, respectively.

Given Z_1, \dots, Z_m are mutually independent, we have

$$G_S(c) = P(Z_S \geq c | \forall S' \in \mathcal{U}(S), G_{S'}(Z_{S'}) \geq \hat{t}^{(\ell_{S'})}(\alpha))$$

Given the definition of $G_S(c)$, we define the rejection path as

$$\mathcal{Q}^{(1:\ell-1)} = \{x : \forall S' \in \mathcal{U}(S), G_{S'}(X_{S'}) \geq \hat{t}^{(\ell_{S'})}(\alpha), \forall S'' \in \mathcal{U}^c(S), G_{S''}(X_{S''}) \leq \hat{t}^{(\ell_{S''})}(\alpha)\} \quad (17)$$

In addition, for two sequence of real numbers a_m and b_m , we write $a_m = o(b_m)$ when $a_m/b_m \rightarrow 0$, and $a_m = O(b_m)$ when $\lim_{m \rightarrow \infty} |a_m/b_m| \leq C$ for some constant C . To prove the asymptotic properties of DART, we need the following lemmas.

Lemma 1. *Under the linear regression model (3), T_i s are asymptotic oracle P-values.*

Lemma 2. *Let $\mathcal{P}_i = \{p \in [0, 1] : P(\tilde{T}_i < p) \geq \epsilon(m)\}$ and $\mathcal{P}'_i = \{p \in [0, 1] : P(\tilde{T}_i < p) \geq \epsilon(m)\epsilon'(m)\}$, with $\epsilon(m), \epsilon'(m) \rightarrow 0$. For any set of independent random variable $\hat{T}_i \in [0, 1]$, and a collection $\mathcal{M} = \{S \subset \{1, \dots, m\} : |S| < c_0\}$ with some constant c_0 ,*

(1) *If $\max_{i \in \mathcal{M}} \sup_{p \in \mathcal{P}'_i} |P(\hat{T}_i < p) / P(\tilde{T}_i < p) - 1| \rightarrow 0$, then,*

$$\sup_{S_0 \in \mathcal{M}} \sup_{p \geq \epsilon(m)} \left| \frac{P(\sum_{i \in S_0} \hat{X}_i > c_{S_0}(p))}{P(\sum_{i \in S_0} \tilde{X}_i > c_{S_0}(p))} - 1 \right| \rightarrow 0,$$

(2) If $\lim_{m \rightarrow \infty} \max_{i \in \mathcal{M}} \sup_{p \in \mathcal{P}'_i} (P(\hat{T}_i < p) / P(\tilde{T}_i < p) - 1) \leq 0$, then,

$$\lim_{m \rightarrow \infty} \sup_{S_0 \in \mathcal{M}} \sup_{p \geq \epsilon(m)} \left(\frac{P(\sum_{i \in S_0} \hat{X}_i > c_{S_0}(p))}{P(\sum_{i \in S_0} \tilde{X}_i > c_{S_0}(p))} - 1 \right) \leq 0$$

Here, $\hat{X}_i = \bar{\Phi}^{-1}(\hat{T}_i)$, $\tilde{X}_i = \bar{\Phi}^{-1}(\tilde{T}_i)$ and $c_{S_0}(p)$ is the value s.t. $P[\sum_{i \in S_0} \tilde{X}_i > c_{S_0}(p)] = p$.

Lemma 3. Let $\tilde{\Omega}_0 = \{i : \tilde{T}_i \text{ follows Unif}(0, 1)\}$, $\mathcal{B}_{0a}^{(\ell)} := \{S \in \mathcal{B}_0^{(\ell)} : \exists A \in \mathcal{A}^{(L)} \setminus \mathcal{A}', \text{ s.t. } S \subset A\}$, and $\mathcal{B}_{0b}^{(\ell)} := \{S \in \mathcal{B}_0^{(\ell)} : S \in \tilde{\Omega}_0\}$, we have:

$$(1) \max_{S \in \mathcal{B}_{0a}^{(\ell)}} \sup_{c \in [0, \gamma_m]} \left| \frac{G_S(c)}{\bar{\Phi}(c)} - 1 \right| \rightarrow 0$$

$$(2) \max_{S \in \mathcal{B}_{0b}^{(\ell)}} \sup_{c \in [0, \bar{\Phi}^{-1}(1/m)]} \left| \frac{P(X_S > c | \mathcal{Q}^{(1:\ell-1)})}{P(X_S > c)} - 1 \right| \rightarrow 0$$

Lemma 4. Define

$$\mathcal{X}^{(\ell)} = \left\{ x : \sum_{S \in \mathcal{B}_0^{(\ell)}} |S| I(T_S < \hat{t}^{(\ell)}) - \sum_{S \in \mathcal{B}_0^{(\ell)}} |S| \hat{t}^{(\ell)} \leq \left\{ \sum_{S \in \mathcal{B}_0^{(\ell)}} |S| \hat{t}^{(\ell)} \right\} \epsilon \right\} \quad (18)$$

$$\mathcal{X}'^{(\ell)} = \left\{ x : \left| \frac{\sum_{S \in \mathcal{B}_0^{(\ell)}} |S| I(T_S < \hat{t}^{(\ell)})}{\sum_{S \in \mathcal{B}_0^{(\ell)}} |S| \hat{t}^{(\ell)}} - 1 \right| \geq \epsilon \right\}$$

Then, $\forall \ell = 1, \dots, L$, when the FDR control holds on layer $1, \dots, \ell - 1$,

(1) For all $\epsilon \in (0, \alpha)$, if $P(m\hat{t}^{(\ell)} \geq Cc_{md}) \rightarrow 1$, then $P(\mathcal{X}^{(\ell)}) = 1 - o(1)$. Together with

$\lim_{m \rightarrow \infty} |\tilde{\Omega}_0|/m = 1$, we have $P(\mathcal{X}'^{(\ell)}) = 1 - o(1)$.

(2) On $\cap_{h=1}^{\ell} \mathcal{X}^{(h)}$, there exist a constant C s.t. $\hat{t}^{(\ell)} \leq Cm^{r_1-1}$.

(3) Let \hat{c}_S be the rejection threshold for the test node $S \in \mathcal{B}^{(\ell)}$, s.t. $\bar{G}_S(\hat{c}_S) = \hat{t}^{(\ell)}$. Then on

$$\cap_{h=1}^{\ell} \mathcal{X}^{(h)},$$

$$\hat{c}_S > \beta_m, \forall S \in \mathcal{B}^{(\ell)},$$

and on $\cap_{h=1}^{\ell-1} \mathcal{X}^{(h)}$,

$$\hat{c}_S < \gamma_m, \forall S \in \mathcal{B}^{(\ell)}.$$

Lemma 5.

$$\frac{\sum_{S \in \mathcal{B}_0^{(\ell)}} |S| \hat{t}^{(\ell)}}{\sum_{S \in \mathcal{B}^{(\ell)}} |S| I(T_S < \hat{t}^{(\ell)})} = \alpha(1 + o(1)) \quad (19)$$

Proof of Theorem 1. Since the proof of the theorem statement (2) is similar to the proof of the theorem statement (1), we will only focusing on the proof of statement (1).

The random variable $FDP^{(\ell)}$ can be decomposed to the product of two parts.

$$FDP^{(\ell)} = \frac{\sum_{S \in \mathcal{B}_0^{(\ell)}} |S| I\{T_S < \hat{t}^{(\ell)}\}}{\sum_{S \in \mathcal{B}_0^{(\ell)}} |S| \hat{t}^{(\ell)}} \times \frac{\sum_{S \in \mathcal{B}_0^{(\ell)}} |S| \hat{t}^{(\ell)}}{\max(\sum_{S \in \mathcal{B}^{(\ell)}} |S| I\{T_S < \hat{t}^{(\ell)}\}, 1)} \quad (20)$$

Based on (20), in order to prove $\lim_{m \rightarrow \infty} P(FDP^{(\ell)} \leq \alpha + \epsilon) = 1$ for all $\epsilon > 0$, we only need prove

$$\lim_{m \rightarrow \infty} P \left\{ \frac{\sum_{S \in \mathcal{B}_0^{(\ell)}} |S| I\{T_S < \hat{t}^{(\ell)}\}}{\sum_{S \in \mathcal{B}_0^{(\ell)}} |S| \hat{t}^{(\ell)}} - 1 < \epsilon \right\} \rightarrow 1 \quad (21)$$

$$\lim_{m \rightarrow \infty} P \left\{ \left| \frac{\sum_{S \in \mathcal{B}_0^{(\ell)}} |S| \hat{t}^{(\ell)}}{\max(\sum_{S \in \mathcal{B}^{(\ell)}} |S| I\{T_S < \hat{t}^{(\ell)}\}, 1)} - \alpha \right| > \epsilon \right\} \rightarrow 0 \quad (22)$$

(22) is immediately followed by Lemma 5, and we will prove (21) by induction. Below is a list of the proof sketch:

1. On layer 1, show $P(m\hat{t}^{(1)} \geq Cc_{\text{md}}) \rightarrow 1$. Then, by applying Lemma 4, we have
 - $P(\mathcal{X}^{(1)}) \rightarrow 1$, which is equivalent to (21). Hence, we proved the FDR control on layer 1.
 - $P(\beta_m < \hat{c}_S < \gamma_m, \forall S \in \mathcal{B}^{(1)}) \rightarrow 1$, and $P(\hat{c}_S < \gamma_m, \forall S \in \mathcal{B}^{(2)}) \rightarrow 1$. Note that although this conclusion is not used to prove the FDR control on the current layer, but is necessary to guarantee the FDR control on higher layers.
2. On layer $\ell \geq 2$, assume the FDR control holds on previous layers and $P(\mathcal{X}^{(\ell')}) \rightarrow 1$ for all $\ell' = 1, \dots, \ell - 1$. Then by Lemma 4, $P(\beta_m < \hat{c}_S < \gamma_m, \forall S \in \cup_{\ell'=1}^{\ell-1} \mathcal{B}^{(\ell')}) \rightarrow 1$, and $P(\hat{c}_S < \gamma_m, \forall S \in \mathcal{B}^{(\ell)}) \rightarrow 1$. Accordingly, we can get $P(m\hat{t}^{(1)} \geq Cc_{\text{md}}) \rightarrow 1$. Then, by applying the Lemma 4 again, we have
 - $P(\mathcal{X}^{(\ell)}) \rightarrow 1$, which is equivalent to (21). Hence, we proved the FDR control on layer ℓ .
 - $P(\beta_m < \hat{c}_S < \gamma_m, \forall S \in \mathcal{B}^{(\ell)}) \rightarrow 1$, and $P(\hat{c}_S < \gamma_m, \forall S \in \mathcal{B}^{(\ell+1)}) \rightarrow 1$.

We start the proof on layer 1.

Layer 1:

Take a subset $\mathcal{F}^{(1)} \subset \mathcal{A}_{\text{md}} \cap \mathcal{A}^{(1)}$, such that $|\mathcal{F}^{(1)}| = c_{\text{md}}$. For any $i \in \mathcal{F}^{(1)}$, we have $P(X_i > \gamma_m) \geq C$. By Markov's inequality, we have:

$$P\left(\left|\sum_{i \in \mathcal{F}^{(1)}} I(X_i > \gamma_m) - \sum_{i \in \mathcal{F}^{(1)}} P(X_i > \gamma_m)\right| \geq c_{\text{md}}^{3/4}\right) \leq C(c_{\text{md}})^{-1/2}$$

Thus,

$$P\left[\sum_{1 \leq i \leq m} I(T_i \leq \hat{t}^{(1)}) \geq Cc_{\text{md}} - c_{\text{md}}^{3/4}\right] \geq 1 - o(1)$$

Therefore, by Lemma 5, exists constant $C^{(1)}$, s.t.

$$P\left[m_0 \hat{t}^{(1)} \geq C^{(1)} c_{\text{md}}\right] \geq 1 - o(1) \quad (23)$$

Together with Lemma 4 (1), we have $P(\mathcal{X}^{(1)}) \rightarrow 1$ and accordingly, $P(FDP^{(1)} < \alpha + \epsilon) \rightarrow 1$.

Layer ℓ :

Based on similar arguments on Layer 1, it is suffice to show $P(m_0 \hat{t}^{(\ell)} > C^{(\ell)} c_{\text{md}}) \rightarrow 1$ for some constant $C^{(\ell)}$.

Assume $\forall h = 1, \dots, \ell - 1$, $P(\mathcal{X}^{(h)}) \rightarrow 1$, then by Lemma 4, we have $P(\beta_m < \hat{c}_S < \gamma_m, \forall S \in \mathcal{B}^{(h)}) \rightarrow 1$, and $P(c_S < \gamma_m, \forall S \in \mathcal{B}^{(\ell)}) \rightarrow 1$.

Let $\mathcal{F}^{(\ell)} \subset \mathcal{A}_{\text{md}} \cap \mathcal{A}^{(\ell)}$ with $|\mathcal{F}^{(\ell)}| = c_{\text{md}}$. Define

$$\hat{\mathcal{F}}^{(\ell)} = \{A \in \mathcal{B}^{(\ell)} \cap \mathcal{F}^{(\ell)} : T_A < \alpha_m\}$$

By condition 2, $\forall A \in \mathcal{F}^{(\ell)}$,

$$P(A \in \hat{\mathcal{F}}^{(\ell)}) \geq P(T_A < \alpha_m, T_D \geq \bar{\Phi}(m^{r_1-1} \sqrt{\log m}), \forall D \in \mathcal{D}(A)) \geq C_1 \quad (24)$$

Accordingly, define $\hat{\mathcal{X}}^{(\ell)} = \{|\hat{\mathcal{F}}^{(\ell)}| \geq c_{\text{md}}/2\}$, then $P(\hat{\mathcal{X}}^{(\ell)}) \geq 1 - o(1)$.

On $\hat{\mathcal{X}}^{(\ell)}$, we have

$$\sum_{S \in \mathcal{B}_1^{(\ell)}} I(T_S \leq \hat{t}^{(\ell)}) \geq C c_{\text{md}}$$

Then based on Lemma 3, we can conclude that $P(m_0 \hat{t}^{(\ell)} \geq C^{(\ell)} c_{\text{md}}) \geq 1 - o(1)$ for some constant $C^{(\ell)}$. \square

Proof of Theorem 2. Let $\mathcal{V}^{(\ell)} = \{S \in \mathcal{B}_0^{(\ell)} : S \subset \mathcal{R}^{(\ell)}\}$ and $\mathcal{W}^{(\ell)} = \{S \in \mathcal{B}_1^{(\ell)} : S \subset \mathcal{R}^{(\ell)}\}$ be the false rejection node set and the rejection node set on layer ℓ , respectively. Define

$$\mathcal{X}_1 = \{S \in \cup_{\ell=2}^L \mathcal{W}^{(\ell)} : S \cap \Omega_{\text{st}}^{(1:L)} \neq \emptyset \text{ and } S \cap \Omega_0 \neq \emptyset\}$$

$$\mathcal{X}_2 = \{S \in \cup_{\ell=2}^L \mathcal{W}^{(\ell)} : S \cap \Omega_{\text{wk}} \neq \emptyset, S \setminus (\Omega_0 \cup \Omega_{\text{wk}}) = \emptyset \text{ and } S \cap \Omega_0 \neq \emptyset\}$$

$$\mathcal{X}_3 = \{S \in \cup_{\ell=2}^L \mathcal{W}^{(\ell)} : S \cap \Omega_1 \setminus (\Omega_{\text{wk}} \cup \Omega_{\text{st}}^{(1:L)}) \neq \emptyset \text{ and } S \cap \Omega_0 \neq \emptyset\}$$

Then,

$$P(\mathcal{X}_1 \neq \emptyset) \leq P(\mathcal{X}_1 \neq \emptyset | \cap_{\ell=1}^L \mathcal{X}^{(\ell)}) P(\cap_{\ell=1}^L \mathcal{X}^{(\ell)}) + P((\cap_{\ell=1}^L \mathcal{X}^{(\ell)})^c) \leq C m^{r_1} o(m^{-r_1}) + o(1) \rightarrow 0$$

$$P(\mathcal{X}_2 \neq \emptyset) \leq P(\mathcal{X}_2 \neq \emptyset | \cap_{\ell=1}^L \mathcal{X}^{(\ell)}) P(\cap_{\ell=1}^L \mathcal{X}^{(\ell)}) + P((\cap_{\ell=1}^L \mathcal{X}^{(\ell)})^c)$$

$$\stackrel{(a)}{\leq} C m^{r_1} P \left[X_S \geq \beta_m \middle| S \in \Omega_{\text{wk}} \cup \Omega_0 \right] + o(1)$$

$$\leq C m^{r_1} o(m^{-r_1}) + o(1) \rightarrow 0$$

Here, the inequality (a) is based on Lemma 4 (1) and (3). By condition 4, $|\mathcal{X}_3| = o(c_{\text{md}})$, accordingly,

$$\begin{aligned} P(FDP > \alpha + \epsilon) &\leq P(\mathcal{X}_1 \cup \mathcal{X}_2 \neq \emptyset) + P \left(\frac{\sum_{\ell=1}^L \sum_{S \in \mathcal{V}^{(\ell)}} |S|}{\sum_{\ell=1}^L \sum_{S \in \mathcal{R}_{\text{node}}^{(\ell)}} |S|} > \alpha + \epsilon, \mathcal{X}_1 \cup \mathcal{X}_2 = \emptyset \right) \\ &\leq o(1) + \sum_{\ell=1}^L P \left(\frac{\sum_{S \in \mathcal{V}^{(\ell)} \setminus \mathcal{X}_3} |S|}{\sum_{S \in \mathcal{R}_{\text{node}}^{(\ell)}} |S|} > \alpha + \epsilon + o(1) \right) \rightarrow 0 \end{aligned}$$

So statement (1) is proved. The statement (2) can be proved in the similar way. \square

Acknowledgment

The microbiome samples were collected and sequenced at Memorial Sloan Kettering Cancer Center (MSKCC) and pre-processed at Duke Cancer Institute (DCI) Bioinformatics Shared Resource (BSR). We thank Tsoni Peled and Marcel van den Brink from MSKCC for their help in sample collection and sequencing. We thank Kouros Owzar and Alexander Sibley from DCI-BSR for the help in data pre-processing and constructive discussions. Xuechan Li and Jichun Xie's research is supported by Jichun Xie's startup fund from Duke University. Anthony Sung's research is supported by NIH Award 1-R01-HL151365.

References

- Aitchison, J., 1982. The statistical analysis of compositional data. *Journal of the Royal Statistical Society: Series B (Methodological)* 44, 139–160.
- Benjamini, Y., Hochberg, Y., 1995. Controlling the false discovery rate: a practical and powerful approach to multiple testing. *Journal of the Royal statistical society: series B (Methodological)* 57, 289–300.
- Cai, T.T., Sun, W., Xia, Y., 2020. Laws: A locally adaptive weighting and screening approach to spatial multiple testing. *Journal of the American Statistical Association* , 1–30.
- Callahan, B.J., McMurdie, P.J., Rosen, M.J., Han, A.W., Johnson, A.J.A., Holmes, S.P., 2016. Dada2: high-resolution sample inference from illumina amplicon data. *Nature methods* 13, 581.
- Claesson, M.J., Jeffery, I.B., Conde, S., Power, S.E., O'connor, E.M., Cusack, S., Harris, H.M., Coakley, M., Lakshminarayanan, B., O'Sullivan, O., et al., 2012. Gut microbiota composition correlates with diet and health in the elderly. *Nature* 488, 178–184.

- Cormen, T.H., Leiserson, C.E., Rivest, R.L., Stein, C., 2001. Introduction To Algorithms. MIT Press. URL: https://books.google.com/books?id=NLngYyWFl_YC&pg=PA370.
- Dmitrienko, A., Tamhane, A.C., 2013. General theory of mixture procedures for gatekeeping. *Biom J* 55, 402–19. doi:10.1002/bimj.201100258.
- Goeman, J.J., Finos, L., 2012. The inheritance procedure: multiple testing of tree-structured hypotheses. *Stat Appl Genet Mol Biol* 11, Article 11. doi:10.1515/1544-6115.1554.
- Guo, W., Lynch, G., Romano, J.P., 2018. A new approach for large scale multiple testing with application to fdr control for graphically structured hypotheses. arXiv preprint arXiv:1812.00258 .
- Hastie, T., Tibshirani, R., Friedman, J., 2009. The elements of statistical learning : data mining, inference, and prediction. Springer.
- Jenq, R.R., Ubeda, C., Taur, Y., Menezes, C.C., Khanin, R., Dudakov, J.A., Liu, C., West, M.L., Singer, N.V., Equinda, M.J., et al., 2012. Regulation of intestinal inflammation by microbiota following allogeneic bone marrow transplantation. *Journal of Experimental Medicine* 209, 903–911.
- Jukes, T.H., Cantor, C.R., et al., 1969. Evolution of protein molecules. *Mammalian protein metabolism* 3, 21–132.
- Kurtz, Z.D., Müller, C.L., Miraldi, E.R., Littman, D.R., Blaser, M.J., Bonneau, R.A., 2015. Sparse and compositionally robust inference of microbial ecological networks. *PLoS computational biology* 11.
- Lee, D., Lee, Y., 2016. Extended likelihood approach to multiple testing with directional error control under a hidden markov random field model. *Journal of Multivariate Analysis* 151, 1 – 13. URL: <http://www.sciencedirect.com/science/article/pii/S0047259X16300458>, doi:<https://doi.org/10.1016/j.jmva.2016.07.001>.

- Li, Y., Hu, Y.J., Satten, G.A., 2020. A bottom-up approach to testing hypotheses that have a branching tree dependence structure, with error rate control. *Journal of the American Statistical Association* , 1–18 URL: <https://doi.org/10.1080/01621459.2020.1799811>, doi:10.1080/01621459.2020.1799811.
- Liu, J., Peissig, P., Zhang, C., Burnside, E., McCarty, C., Page, D., 2012. Graphical-model based multiple testing under dependence, with applications to genome-wide association studies. *Uncertain Artif Intell* 2012, 511–522.
- Liu, W., et al., 2013. Gaussian graphical model estimation with false discovery rate control. *The Annals of Statistics* 41, 2948–2978.
- Meijer, R.J., Goeman, J.J., 2015. A multiple testing method for hypotheses structured in a directed acyclic graph. *Biom J* 57, 123–43. doi:10.1002/bimj.201300253.
- Schliep, K., 2011. phangorn: phylogenetic analysis in r. *Bioinformatics* 27, 592–593. URL: <https://doi.org/10.1093/bioinformatics/btq706>.
- Shu, H., Nan, B., Koeppe, R., 2015. Multiple testing for neuroimaging via hidden markov random field. *Biometrics* 71, 741–750.
- Soriano, J., Ma, L., 2017. Probabilistic multi-resolution scanning for two-sample differences. *Journal of The Royal Statistical Society Series B-statistical Methodology* 79, 547–572.
- Sun, W., Cai, T., 2009. Large-scale multiple testing under dependence. *Journal of the Royal Statistical Society: Series B (Statistical Methodology)* 71, 393–424.
- Xie, J., Li, R., 2018. False discovery rate control for high dimensional networks of quantile associations conditioning on covariates. *J R Stat Soc Series B Stat Methodol* 80, 1015–1034. doi:10.1111/rssb.12288.
- Yekutieli, D., 2008. Hierarchical false discovery rate-controlling methodology. *Journal of the*

American Statistical Association 103, 309–316. URL: <http://www.jstor.org/stable/27640041>.

Zhang, C., Fan, J., Yu, T., 2011. Multiple testing via FDR_L for large scale imaging data. *Annals of statistics* 39, 613.

Supplementary Materials for "Distance Assisted Recursive Testing"

In this supplementary files, we provided the detailed algorithms of DART, the tuning parameter selection rule, numerical evaluation of setting M as infinity, and the proofs of the lemmas.

S1 Algorithm Pseudo Codes

S1.1 Stage I: Transform the distance matrix into an aggregation tree

Algorithm 1: DART Stage I. Transform the distance matrix into an aggregation tree.

Data: distance matrix $D = (d_{ij})_{m \times m}$, the maximum layer L , the maximum children number M , the maximum distance threshold $g^{(2)}, \dots, g^{(L)}$.

Result: an aggregation tree $\mathcal{T}_L = \{\mathcal{A}^{(\ell)} : \ell \in \{1, \dots, L\}\}$ and $\mathcal{C}(A)$ for all $A \in \mathcal{A}^{(\ell)}$ and all $\ell \in \{1, \dots, L\}$.

$\ell = 1, \mathcal{A}^{(1)} = \{\{1\}, \dots, \{m\}\},$

for $A \in \mathcal{A}^{(1)}$ **do** $\mathcal{C}(A) = \emptyset$ // Remark 1

for $\ell \in \{2, \dots, L\}$ **do** // Remark 2

$\mathcal{A}^{(\ell)} = \emptyset, \tilde{\mathcal{A}} = \mathcal{A}^{(\ell-1)}, \text{dist}^{(\ell)}(A_1, A_2) = \text{dist}(A_1, A_2), \forall A_1, A_2 \in \tilde{\mathcal{A}}$ // Remark 3

while $|\tilde{\mathcal{A}} \setminus \mathcal{A}^{(\ell)}| > 0$ **do**

$(\check{A}_1, \check{A}_2) = \arg \min_{A_1 \in \tilde{\mathcal{A}}, A_2 \in \tilde{\mathcal{A}} \setminus \{A_1\}} \text{dist}^{(\ell)}(A_1, A_2)$ // Remark 4

if $\text{dist}^{(\ell)}(\check{A}_1, \check{A}_2) > g^{(\ell)}$ **then** // Remark 5

for $A \in \tilde{\mathcal{A}} \setminus \mathcal{A}^{(\ell)}$ **do** $\mathcal{C}(A) = A, \mathcal{A}^{(\ell)} = \mathcal{A}^{(\ell)} \cup \{A\}, \tilde{\mathcal{A}} = \tilde{\mathcal{A}} \setminus \{A\}$

else

$\check{\mathcal{A}} = \check{A}_1 \cup \check{A}_2$

for $i \in \{1, 2\}$ **do** // Remark 6

if $\check{A}_i \in \mathcal{A}^{(\ell)}$ **then** $\mathcal{C}_i = \mathcal{C}(\check{A}_i)$ **else** $\mathcal{C}_i = \{\check{A}_i\}$

$\mathcal{C}(\check{\mathcal{A}}) = \mathcal{C}_1 \cup \mathcal{C}_2$

if $|\mathcal{C}(\check{\mathcal{A}})| < M$ **then**

$\mathcal{A}^{(\ell)} = \mathcal{A}^{(\ell)} \cup \{\check{\mathcal{A}}\} \setminus \{\check{A}_1, \check{A}_2\}, \tilde{\mathcal{A}} = \tilde{\mathcal{A}} \cup \{\check{\mathcal{A}}\} \setminus \{\check{A}_1, \check{A}_2\}$

else if $|\mathcal{C}(\check{\mathcal{A}})| = M$ **then**

$\mathcal{A}^{(\ell)} = \mathcal{A}^{(\ell)} \cup \{\check{\mathcal{A}}\} \setminus \{\check{A}_1, \check{A}_2\}, \tilde{\mathcal{A}} = \tilde{\mathcal{A}} \setminus \{\check{A}_1, \check{A}_2\}$

else

$\text{dist}^{(\ell)}(\check{A}_1, \check{A}_2) = +\infty$ // Remark 7

To obtain such an aggregation tree, we develop Algorithm 1 with remarks listed below.

Remark 1. On layer 1, we set up each node as a single feature node. All these nodes have empty children sets.

Remark 2. On layer ℓ , we aggregate nodes from layer $\ell - 1$ to form new nodes on this layer.

Remark 3. At the beginning of layer ℓ , $\mathcal{A}^{(\ell)}$ is set as the empty set, and it will be updated during the aggregation process. $\tilde{\mathcal{A}}$ is the candidate node set with all the nodes that can possibly be aggregated. It may contain the layer $\ell - 1$'s nodes that have not be aggregated yet and layer ℓ 's nodes that have already been aggregated but can possibly be further aggregated. The layer ℓ distance between $A_1, A_2 \in \tilde{\mathcal{A}}$ is denoted by $\text{dist}^{(\ell)}(A_1, A_2)$. We set it equals to $\text{dist}(A_1, A_2)$, which is defined in section 2.2.1.

Remark 4. We use the greedy algorithm to select the closest two nodes \check{A}_1 and \check{A}_2 from the current candidate node set $\tilde{\mathcal{A}}$. If there exists a tie, we select the first node pair that reaches the minimal distance. For example, in Figure 1b, at the beginning of layer 2, $\text{dist}(\{1\}, \{2\}) = 2$ reaches the minimal distance among all node pairs on layer 1, so they will be selected to be further considered for aggregation.

Remark 5. We check if $\text{dist}(\check{A}_1, \check{A}_2) > g^{(\ell)}$. If yes, the remaining candidate nodes are too far away from each other and will not be further aggregated. Then the remaining child nodes on layer $\ell - 1$ will be kept on layer ℓ , and the aggregation on layer ℓ ends. If not, \check{A}_1 and \check{A}_2 will be further considered for aggregation.

Remark 6. We define the new node $\check{A} = \check{A}_1 \cup \check{A}_2$. $\mathcal{C}(\check{A})$ depends on the identity of \check{A}_1 and \check{A}_2 : if \check{A}_i is a candidate child on layer $\ell - 1$, then itself will be included in $\mathcal{C}(\check{A})$; otherwise, \check{A}_i 's children will be included in $\mathcal{C}(\check{A})$.

Remark 7. We check the number of children of \check{A} . If $|\mathcal{C}(\check{A})| < M$, we add \check{A} to $\mathcal{A}^{(\ell)}$ and remove \check{A}_1 and \check{A}_2 , and change $\tilde{\mathcal{A}}$ correspondingly. If $|\mathcal{C}(\check{A})| = M$, we change $\mathcal{A}^{(\ell)}$ in the same way when $|\mathcal{C}(\check{A})| < M$, and remove \check{A}_1 and \check{A}_2 from $\tilde{\mathcal{A}}$ to prevent them being selected again. This step also guarantees the number of children of a node $A \in \tilde{\mathcal{A}}$ is always smaller than M . If $|\mathcal{C}(\check{A})| > M$, we just reset the layer ℓ distance between \check{A}_1 and \check{A}_2 to be $+\infty$, so that they will never be aggregated on layer ℓ , but still have chance to aggregate with other nodes in $\tilde{\mathcal{A}}$.

S1.2 Stage II: Embed multiple testing in the tree

Algorithm 2: DART Stage II. Embed multiple testing in the tree.

Data: Tree $\mathcal{T}_L = \{\mathcal{A}^{(i)} : i = 1, \dots, L\}$, P-values (T_1, \dots, T_m) , and FDR level α .

Result: The set of rejected features R_{feat} .

Set $\hat{t}^{(1)}$ as in (6), $R_{\text{feat}} = \{i : T_i \leq \hat{t}^{(1)}\}$ // *Multiple testing on layer 1.*

for $\ell \in \{2, \dots, L\}$ **do** // *Testing recursively on higher layers*

$k = 0, T = \text{NULL}$

for $S_k \in \mathcal{B}^{(\ell)}$ **do**

$k = k + 1, X_{S_k} = \sum_{j \in S_k} \bar{\Phi}^{-1}(T_j) / \sqrt{|S_k|}$

$T = (T, \bar{\Phi}(X_{S_k}))'$ // *Append the new working P-value at the end*

Set $\hat{t}^{(\ell)}$ as in (8), $R_{\text{node}}^{(\ell)} = \{S_{k'} : T_{k'} < \hat{t}^{(\ell)}\}$, $R_{\text{feat}} = R_{\text{feat}} \cup \{\cup_{S \in R_{\text{node}}^{(\ell)}} S\}$

S2 Numerical experiments

S2.1 Simulated Settings

Before we display the five settings, we first introduce the following notations that are used across all five settings:

$$\eta_{1,i} = \{[2\phi_1(d_{22,i}) - 0.2] \vee 0\} + \{\phi_2(d_{7,i})\};$$

$$\eta_{2,i} = \{[3.4\phi_3(d_{156,i}) - 0.8] \vee 0\} + 3\{\phi_4(d_{7,i})\}$$

$$+ 10 * I(i \in \{100, 200, 300, 400, 500, 600, 700, 800, 900, 1000\}),$$

where ϕ_1, ϕ_2, ϕ_3 and ϕ_4 are the PDF of $N(0, 1), N(0, 0.1), N(0, 0.8)$ and $N(0, 0.05)$, respectively.

SE1: For node $i \in \{1, \dots, m\}$, the feature P-value $T_i = 2\bar{\Phi}(|\check{Z}_i|)$, where the $\check{Z}_1, \dots, \check{Z}_m$ are independently generated from $N(\sqrt{n}\theta_i, 1)$, with

$$\theta_i = \begin{cases} \frac{1}{2}\eta_{1,i}I(\eta_{1,i} - 0.15 > 0), & (n, m) = (90, 100) \\ \frac{1}{7}\eta_{2,i}I(\eta_{2,i} - 0.15 > 0), & (n, m) = (300, 1000). \end{cases}$$

SE2: For node $i \in \{1, \dots, m\}$, the feature P-value $T_i = 2\bar{\Phi}(|\check{Z}_i|)$, where the $\check{Z}_1, \dots, \check{Z}_m$ are independently generated from a mixture distribution $0.04\text{Laplace}(\sqrt{n}\theta_i, 1) + 0.96\text{N}(\sqrt{n}\theta_i, 1)$ with

$$\theta_i = \begin{cases} \frac{2}{5}\eta_{1,i}I(\eta_{1,i} - 0.15 > 0), & (n, m) = (90, 100) \\ \frac{2}{13}\eta_{2,i}I(\eta_{2,i} - 0.15 > 0), & (n, m) = (300, 1000) \end{cases}$$

SE3: For node $i \in \{1, \dots, m\}$, the feature P-value $T_i = 2\bar{\Phi}(|\check{Z}_i|)$, where the $\check{Z}_1, \dots, \check{Z}_m$ are independently generated from the mixture distribution with $0.04t_5(\sqrt{n}\theta_i) + 0.95\text{N}(\sqrt{n}\theta_i, 1)$. Here, $t_5(\sqrt{n}\theta_i)$ stands for the student t distribution with 5 degree of freedom and none centrality parameter $\sqrt{n}\theta_i$, with

$$\theta_i = \begin{cases} \frac{1}{3}\eta_{1,i}I(\eta_{1,i} - 0.15 > 0), & (n, m) = (90, 100) \\ \frac{2}{13}\eta_{2,i}I(\eta_{2,i} - 0.15 > 0), & (n, m) = (300, 1000) \end{cases}$$

SE4: Consider the linear mode defined in (3), with $p_0 = 3$, and $\sigma = 1$. In model (3), $W_1 = 1$ is the intercept term, W_2 and W_3 are sampled from $\text{Binom}(0.5)$ and $\text{Unif}(0.1, 0.5)$, respectively. Also let $\theta_{1,i} = \theta_{3,i} = 0.1$ and

$$\theta_i = \theta_{1,i} = \begin{cases} 2\eta_{1,i}I(\eta_{1,i} - 0.15 > 0), & (n, m) = (90, 100) \\ \frac{5}{6}\eta_{2,i}I(\eta_{2,i} - 0.15 > 0), & (n, m) = (300, 1000) \end{cases}$$

The feature P-value T_i is defined in (4).

SE5: Consider the cox regression model

$$\lambda_i(t) = \lambda_{0i}(t) \exp\{\theta_{1,i}W_1 + \theta_{2,i}W_2\}$$

Where $\lambda_i(t)$ and $\lambda_{0i}(t)$ is the hazard and baseline hazard at time t , respectively. Set $\theta_{0,i} = \theta_{2,i} = 0.1$ and

$$\theta_i = \theta_{1,i} = \begin{cases} \frac{4}{5}\eta_{1,i}I(\eta_{1,i} - 0.15 > 0), & (n, m) = (90, 100) \\ \frac{2}{7}\eta_{2,i}I(\eta_{2,i} - 0.15 > 0), & (n, m) = (300, 1000) \end{cases}$$

The covariates W_1 and W_2 are sampled from $\text{Binom}(0.5)$ and $\text{Unif}(0.1, 0.5)$, respec-

tively. The event time is generated from the exponential distribution with rate $\exp\{\theta_{1,i}W_1 + \theta_{2,i}W_2\}$, and the censoring time is sampled from $\text{Unif}(0, 5)$. The feature P-value T_i is obtained from the Wald test.

S2.2 Tuning parameter selection for applying DART on simulated data

The section 2.3 introduces the tuning parameter selection for the aggregation tree construction. Based on it, the tuning parameter for our numerical study is selected as follow:

- If $(n, m) = (90, 100)$: Based on recommendation in section 2.3, we choose $M = 3$ and construct a $L = \lceil \log_M 100 - \log_M 30 \rceil = 2$ layers aggregation tree. We use Algorithm 3 to construct a dynamic set G and search the value $g^{(2)}$. Table S1 (1) tracks the number of non-single-child nodes $|\tilde{A}^{(2)}(g)|$ based on different values of $g \in G$. By applying the algorithm,

$$g^{(2)} = 26 / \sqrt{n \log m \log \log m}$$

- If $(n, m) = (300, 1000)$: Similar to the previous case, we choose $M = 3$ and construct a $L = \lceil \log_M 1000 - \log_M 30 \rceil = 4$ layers aggregation tree. Based on Algorithm 3, we have Table S1 which tracks the number of non-single-child nodes on each layer, and,

$$g^{(2)} = \frac{8}{\sqrt{n \log m \log \log m}}, g^{(3)} = \frac{22}{\sqrt{n \log m \log \log m}}, g^{(4)} = \frac{56}{\sqrt{n \log m \log \log m}}$$

Algorithm 3: $g^{(\ell)}$ Selection algorithm.

Data: Distance Matrix $D = (d_{ij})_{m \times m}$, Sample size n , number of features m , the maximum children number M , the maximum layer L

Result: $g^{(2)}, \dots, g^{(L)}$.

// set searching upper bound d_{\max} and step-size $s_{n,m}$

Let $d_{\max} = \max_{j \in \Omega} \min_{i \in \{i: i \neq j\}} d_{ij}$; $s_{n,m} = 2/\sqrt{n \log(m) \log \log(m)}$;

for $\ell = 2, \dots, L$ **do**

// on layer ℓ , search $g^{(\ell)}$ from $(g^{(\ell-1)}, d_{\max}]$, $g^{(1)} = 0$

Let $M_g = \text{NULL}$; $e_g = 1$; $G = \text{NULL}$; $g = g^{(\ell-1)} + s_{n,m}$;

while $g \leq (2M^{L-2} - 1)d_{\max}$ **and** $e_g < 10$ **do**

// stop searching process if the value g exceed the searching upper bound or the $|\tilde{A}^{(\ell)}(g)|$ does not increase for past 10 candidate values g .

// stop searching process if the value g exceed the searching upper bound.

Use Algorithm 1 to Construct an ℓ layers aggregation tree

$\mathcal{T}_\ell = \{\mathcal{A}^{(\ell')}: \ell' = 1, \dots, \ell\}$ with maximum children number M , and $(g^{(1)}, \dots, g^{(\ell-1)}, g)$;

Set $\tilde{A}^{(\ell)}(g) = \{A: A \in \mathcal{A}^{(\ell)}(g), |\mathcal{C}(A)| \geq 2\}$; **if** $m_g \geq |\tilde{A}^{(\ell)}(g)|$ **then**

$e_g = e_g + 1$;

else

$e_g = 1$;

$G = (G, g)$; $M_g = (M_g, |\tilde{A}^{(\ell)}(g)|)$; $m_g = |\tilde{A}^{(\ell)}(g)|$;

$g = g + s_{n,m}$;

$g^{(\ell)} = \min\{\arg \max_{g \in G} M_g\}$;

Table S1: The number of non-single-child nodes based on value $g \in G$ when $M = 3$. For simplicity purpose, the value g is represented by its nominator: $g' = g \times \sqrt{n \log m \log \log m}$. The selected g' and its corresponding $|\tilde{\mathcal{A}}^{(2)}(g)|$ is highlighted in bold.

(1) $(n, m) = (90, 100)$:

Layer 2	g'	2	4	6	8	10	12	14	16	18	20	22	24	26	28	30	32	...
	$ \tilde{\mathcal{A}}^{(3)}(g) $	5	10	17	22	29	31	31	39	40	40	40	40	41	41	41	41	...

(2) $(n, m) = (300, 1000)$:

Layer 2	g'	2	4	6	8	10	12	14	16	...							
	$ \tilde{\mathcal{A}}^{(2)}(g) $	49	149	245	293	293	293	293	293	...							
Layer 3	g'	10	12	14	16	18	20	22	24	26	28	30	...				
	$ \tilde{\mathcal{A}}^{(3)}(g) $	103	154	191	221	230	239	241	241	241	241	241	...				
Layer 4	g'	...	38	40	42	44	46	48	50	52	54	56	58	60	62	64	...
	$ \tilde{\mathcal{A}}^{(4)}(g) $...	116	118	119	120	120	120	120	120	120	121	121	121	121	121	...

S3 Additional numerical results for assessing impact of the parameter M

In this section, we numerically investigate the impact of the choice of M by comparing the numerical results when $M = 3$ and $M = \infty$. When $M = 3$, the tuning parameters are same to the parameters in 2.3. When $M = \infty$, in order to have a relatively fair comparison, we set the same total layer L as the value in 2.3. The selection procedure of $g^{(\ell)}$ is similar to 2.3. Based on the Algorithm 3, we have

- If $(n, m) = (90, 100)$: we set $g^{(2)} = \frac{16}{\sqrt{n \log m \log \log m}}$
- If $(n, m) = (300, 1000)$: we set $g^{(2)} = \frac{12}{\sqrt{n \log m \log \log m}}$, $g^{(3)} = \frac{26}{\sqrt{n \log m \log \log m}}$ and $g^{(4)} = \frac{44}{\sqrt{n \log m \log \log m}}$.

Figure S1 compares the performance between two different M values under SE1-SE5. We only compare the performance on the top layer of the aggregation tree. Based on the figure, our method is still valid with FDR control when $M = \infty$.

Table S2: The number of non-single-child nodes based on value $g \in G^{(\ell)}$ when $M = \infty$. For simplicity purpose, the value g is represented by its nominator: $g' = g \times \sqrt{n \log m \log \log m}$. The selected g' and its corresponding $|\tilde{\mathcal{A}}^{(\ell)}(g)|$ is highlighted in bold.

(1) $(n, m) = (90, 100)$:

Layer 2	g'	2	4	6	8	10	12	14	16	18	20	22	24	...
	$ \tilde{\mathcal{A}}^{(2)}(g) $	5	10	17	22	29	30	30	35	32	31	29	28	...

(2) $(n, m) = (300, 1000)$:

Layer 2	g'	2	4	6	8	10	12	14	16	18	20	...			
	$ \tilde{\mathcal{A}}^{(2)}(g) $	49	149	239	291	300	303	295	288	263	245	...			
Layer 3	g'	14	16	18	20	22	24	26	28	30	32	34	...		
	$ \tilde{\mathcal{A}}^{(3)}(g) $	53	101	130	148	163	167	169	166	159	152	144	...		
Layer 4	g'	28	30	32	34	36	38	40	42	44	46	48	50	52	...
	$ \tilde{\mathcal{A}}^{(4)}(g) $	17	33	47	56	66	70	74	76	80	79	79	79	77	...

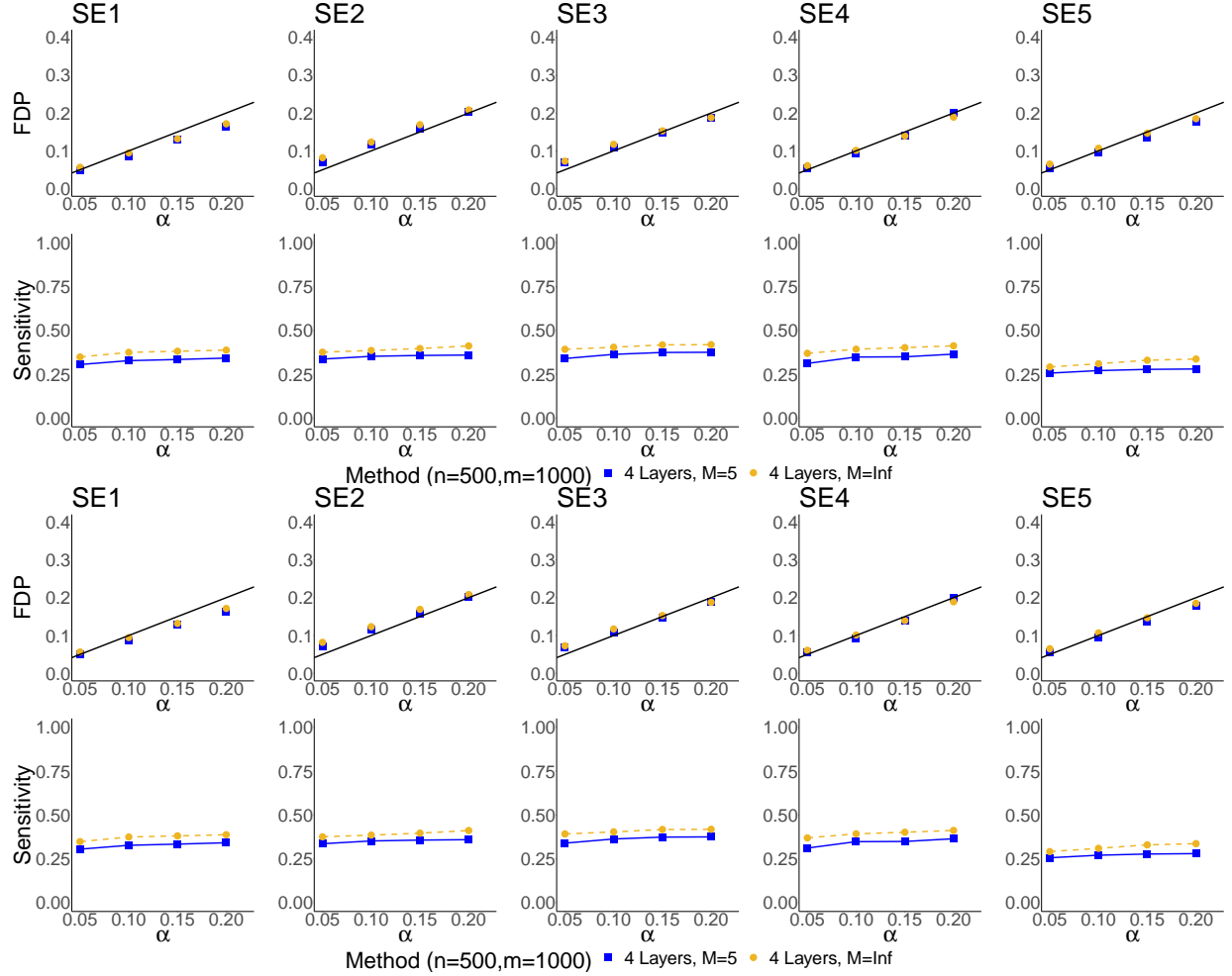


Figure S1: Additional simulation results for setting SE1-SE5. The first two rows represent the results in the setting $(n, m) = (90, 100)$, and the second two rows represent the results in the setting $(n, m) = (300, 1000)$.

S4 Proof of the Lemmas

Proof of Lemma 1. Let $X_i'^* = \frac{\mathbf{q}^T \hat{\boldsymbol{\theta}}_i}{s \sqrt{\mathbf{q}^T (\mathcal{W}^T \mathcal{W})^{-1} \mathbf{q}}}$ and $X_{o,i}' = \frac{\mathbf{q}^T \hat{\boldsymbol{\theta}}_i}{\sigma \sqrt{\mathbf{q}^T (\mathcal{W}^T \mathcal{W})^{-1} \mathbf{q}}}$, we have $X_{o,i}' \sim N(\eta_i, 1)$ with $\eta_i = \frac{\mathbf{q}^T \boldsymbol{\theta}_i}{\sigma \sqrt{\mathbf{q}^T (\mathcal{W}^T \mathcal{W})^{-1} \mathbf{q}}}$.

To show the statistics T_i is asymptotically oracle, it is suffice to show:

$$P(|\Phi^{-1}(T_i) - \Phi^{-1}(\tilde{T}_i)| > (\log m)^{-2.5}) = o((\log m)^{-1})$$

Given

$$\begin{aligned}
|\Phi^{-1}(T_i) - \Phi^{-1}(\tilde{T}_i)| &\leq \sup_{x \geq 0} \frac{\phi(x)}{\phi[\Phi^{-1}(2\Phi(-x))]} ||X_i'^*| - |X'_{o,i}|| \\
&\leq |X_i'^* - X'_{o,i}| \\
&= |X'_{o,i}(\sigma/s - 1)|
\end{aligned}$$

and based on condition 1,

$$P\left(|X'_{o,i}(\sigma/s - 1)| > (\log m)^{-2.5}\right) \leq P(|X'_{o,i}| > \sqrt{\log m}) + P(|\sigma/s - 1| > (\log m)^{-3})$$

It is suffice to show

$$P(|\sigma/s - 1| > (\log m)^{-3}) = o((\log m)^{-1}) \quad (\text{S1})$$

Let $Y_1, \dots, Y_{n-p_0-1} \stackrel{iid}{\sim} \mathcal{X}^2(1)$ and $Y = \sum_{k=1}^{n-p_0-1} (Y_k - 1) / \sqrt{2(n-p_0-1)}$, we have $Y / \sqrt{n-p_0-1} \sim \mathcal{X}^2(n-p_0-1) / (n-p_0-1) - 1$. Since $s^2/\sigma^2 \sim \mathcal{X}^2(n-p_0-1) / (n-p_0-1)$, based on Lemma 6.1 in Liu et al. (2013),

$$P(|s/\sigma - 1| > (\log m)^{-3}) \leq P(|s^2/\sigma^2 - 1| > (\log m)^{-3}) = o((\log m)^{-1})$$

Thus, after trivial calculation, the equation (S1) holds. \square

Proof of Lemma 2. (1) Define $\tilde{X}_i = \bar{\Phi}(\tilde{T}_i)$, For $k \in \{1, \dots, c_0\}$, let $q_0 \geq \epsilon(m)$. Also define $b_{1,k}(q_0)$, c_1, \dots, c_k be the value s.t. $P(\sum_{j=1}^k \tilde{X}_j > b_{1,k}(q_0)) = q_0 [\epsilon'(m)]^{(c_0-k)/c_0}$, and $P(\tilde{X}_1 > c_1) = \dots = P(\tilde{X}_k > c_k) = \epsilon(m)\epsilon'(m)$, respectively. For simplicity sake, we use $b_{1,k}$ to present $b_{1,k}(q_0)$.

Based on the definition, we have

$$b_{1,k} < \sum_{j=1}^k c_j$$

Thus, when $k = 2$,

$$\begin{aligned}
& P(\hat{X}_1 + \hat{X}_2 > b_{1,2}) \\
&= P(\hat{X}_1 + \hat{X}_2 > b_{1,2}, \hat{X}_1 > b_{1,2} - c_2, \hat{X}_2 > b_{1,2} - c_1) \\
&\quad + P(\hat{X}_1 + \hat{X}_2 > b_{1,2}, \hat{X}_1 < b_{1,2} - c_2) + P(\hat{X}_1 + \hat{X}_2 > b_{1,2}, \hat{X}_2 < b_{1,2} - c_1) \\
&= P(\hat{X}_1 + \hat{X}_2 > b_{1,2}, c_1 > \hat{X}_1 > b_{1,2} - c_2) + P(\hat{X}_1 > c_1, \hat{X}_2 > b_{1,2} - c_1) \\
&\quad + P(\hat{X}_1 + \hat{X}_2 > b_{1,2}, \hat{X}_1 < b_{1,2} - c_2) + P(\hat{X}_1 + \hat{X}_2 > b_{1,2}, \hat{X}_2 < b_{1,2} - c_1)
\end{aligned}$$

Based on construction, the last three terms always smaller than $\epsilon(m)\epsilon'(m)(1 + \delta_4(m))$ for

$$\delta_4(m) := \max_{i \in \Omega} \sup_{p \in \mathcal{P}'_i} \left| P(\hat{T}_i < p) / P(\tilde{T}_i < p) - 1 \right| \rightarrow 0, \text{ and accordingly, we have}$$

$$\begin{aligned}
& P(\hat{X}_1 + \hat{X}_2 > b_{1,2}, c_1 > \hat{X}_1 > b_{1,2} - c_2) + P(\hat{X}_1 > c_1, \hat{X}_2 > b_{1,2} - c_1) \\
&\leq [P(\hat{X}_1 + \tilde{X}_2 > b_{1,2}, c_1 > \hat{X}_1 > b_{1,2} - c_2) + P(\hat{X}_1 > c_1, \tilde{X}_2 > b_{1,2} - c_1)](1 + \delta_4(m)) \\
&\leq [P(\hat{X}_1 + \tilde{X}_2 > b_{1,2}, \hat{X}_1 > b_{1,2} - c_2, \tilde{X}_2 > b_{1,2} - c_1)](1 + \delta_4(m)) \\
&\leq P(\tilde{X}_1 + \tilde{X}_2 > b_{1,2}, \tilde{X}_1 > b_{1,2} - c_2, \tilde{X}_2 > b_{1,2} - c_1)(1 + \delta_4(m))^2
\end{aligned}$$

Based on similar arguments, we can also have

$$\begin{aligned}
& P(\hat{X}_1 + \hat{X}_2 > b_{1,2}, c_1 > \hat{X}_1 > b_{1,2} - c_2) + P(\hat{X}_1 > c_1, \hat{X}_2 > b_{1,2} - c_1) \\
&\geq P(\tilde{X}_1 + \tilde{X}_2 > b_{1,2}, \tilde{X}_1 > b_{1,2} - c_2, \tilde{X}_2 > b_{1,2} - c_1)(1 - \delta_4(m))^2
\end{aligned}$$

Thus,

$$\sup_{q_0 \geq \epsilon(m)} \left[\epsilon'(m) \right]^{\frac{c_0 - 2}{c_0}} \left| \frac{P(\hat{X}_1 + \hat{X}_2 > b_{1,2})}{P(\tilde{X}_1 + \tilde{X}_2 > b_{1,2})} - 1 \right| \rightarrow 0$$

Similarly, if $\sup_{q_0 \geq \epsilon(m)} \left[\epsilon'(m) \right]^{\frac{c_0 - k}{c_0}} \left| \frac{P(\sum_{j=1}^k \hat{X}_j > b_{1,k})}{P(\sum_{j=1}^k \tilde{X}_j > b_{1,k})} - 1 \right| \rightarrow 0$, we can have

$$\sup_{q_0 \geq \epsilon(m)} \left[\epsilon'(m) \right]^{\frac{c_0 - k - 1}{c_0}} \left| \frac{P(\sum_{j=1}^{k+1} \hat{X}_j > b_{1,k+1})}{P(\sum_{j=1}^{k+1} \tilde{X}_j > b_{1,k+1})} - 1 \right| \rightarrow 0$$

Thus, we can get (1). In addition, based on the similar arguments, we can get (2).

□

Proof of Lemma 3. (1) Let $Z'_1, \dots, Z'_K \stackrel{iid}{\sim} N(0, 1)$, with $2 \leq K < M^{L-1}$. Define the set $\mathfrak{M} = \{\mathcal{M}_1 \subset \{1, \dots, m\} : 1 \leq |\mathcal{M}_1| \leq K-1\}$. It is suffice to show:

$$\lim_{m \rightarrow \infty} \sup_{\mathcal{M}_1 \in \mathfrak{M}} \sup_{\substack{c_1 \in [\beta_0, \gamma_m] \\ c_2 \in [0, \gamma_m]}} \frac{P\left(\frac{1}{\sqrt{K}} \sum_{i=1}^K Z'_i > c_2, \frac{1}{\sqrt{|\mathcal{M}_1|}} \sum_{j \in \mathcal{M}_1} Z'_j > c_1\right)}{P\left(\frac{1}{\sqrt{K}} \sum_{i=1}^K Z'_i > c_2\right)} = 0$$

Here, $\beta_0 = \sqrt{2b(1-r_1) \log m + b(1-r_1) \log \log \log m}$, with

$$b = \frac{\frac{2M^{L-1}+1}{M^{L-1}+1} - r_1}{2(1-r_1)} \in \left(\frac{M^{L-1}}{(M^{L-1}+1)(1-r_1)}, 1 \right).$$

For simplification, let $k_1 = |\mathcal{M}_1|$. For Z_1 and $Z_2 \stackrel{iid}{\sim} N(0, 1)$, define

$$\mathcal{D}_m = \left\{ c_2 \in (0, \gamma_m) : \frac{d}{dc_2} \frac{P\left(\sqrt{\frac{k_1}{K}} Z_1 + \sqrt{\frac{K-k_1}{K}} Z_2 > c_2, Z_1 > \beta_0\right)}{P\left(\sqrt{\frac{k_1}{K}} Z_1 + \sqrt{\frac{K-k_1}{K}} Z_2 > c_2\right)} = 0 \right\}$$

, then

$$\begin{aligned} & \sup_{\substack{c_1 \in [\beta_0, \gamma_m] \\ c_2 \in [0, \gamma_m]}} \frac{P\left(\frac{1}{\sqrt{K}} \sum_{i=1}^K Z'_i > c_2, \frac{1}{\sqrt{|\mathcal{M}_1|}} \sum_{j \in \mathcal{M}_1} Z'_j > c_1\right)}{P\left(\frac{1}{\sqrt{K}} \sum_{i=1}^K Z'_i > c_2\right)} \\ & \leq 2 \sup_{c_2 \in [0, \gamma_m]} \frac{P\left(\sqrt{\frac{k_1}{K}} Z_1 + \sqrt{\frac{K-k_1}{K}} Z_2 > c_2, Z_1 > \beta_0\right)}{P\left(\sqrt{\frac{k_1}{K}} Z_1 + \sqrt{\frac{K-k_1}{K}} Z_2 > c_2\right)} \\ & \leq 2 \max \left\{ \max_{c_2=0 \text{ or } \gamma_m} \frac{P\left(\sqrt{\frac{k_1}{K}} Z_1 + \sqrt{\frac{K-k_1}{K}} Z_2 > c_2, Z_1 > \beta_0\right)}{P\left(\sqrt{\frac{k_1}{K}} Z_1 + \sqrt{\frac{K-k_1}{K}} Z_2 > c_2\right)}, \right. \\ & \quad \left. \sup_{c_2 \in \mathcal{D}_m} \frac{P\left(\sqrt{\frac{k_1}{K}} Z_1 + \sqrt{\frac{K-k_1}{K}} Z_2 > c_2, Z_1 > \beta_0\right)}{P\left(\sqrt{\frac{k_1}{K}} Z_1 + \sqrt{\frac{K-k_1}{K}} Z_2 > c_2\right)} \right\} \end{aligned}$$

(i). When $c_2 = 0$,

$$\lim_{m \rightarrow \infty} \frac{P\left(\sqrt{\frac{k_1}{K}} Z_1 + \sqrt{\frac{K-k_1}{K}} Z_2 > c_2, Z_1 > \beta_0\right)}{P\left(\sqrt{\frac{k_1}{K}} Z_1 + \sqrt{\frac{K-k_1}{K}} Z_2 > c_2\right)} = \lim_{m \rightarrow \infty} 2P\left(\sqrt{\frac{k_1}{K}} Z_1 + \sqrt{\frac{K-k_1}{K}} Z_2 > c_2, Z_1 > \beta_0\right) = 0$$

(ii). When $c_2 = \gamma_m$, $c_2/\beta_0 = \sqrt{\frac{1}{b(1-r_1)}}$,

$$\begin{aligned} & \lim_{m \rightarrow \infty} \frac{P(\sqrt{\frac{k_1}{K}}Z_1 + \sqrt{\frac{K-k_1}{K}}Z_2 > c_2, Z_1 > \beta_0)}{P(\sqrt{\frac{k_1}{K}}Z_1 + \sqrt{\frac{K-k_1}{K}}Z_2 > c_2)} = \lim_{\beta_0 \rightarrow \infty} \frac{\int_{\beta_0}^{\infty} \int_{S\sqrt{\frac{K}{K-k_1}}\beta_0 - \sqrt{\frac{k_1}{K-k_1}}z_1}^{\infty} \phi(z_1)\phi(z_2)dz_2dz_1}{\int_{S\beta_0}^{\infty} \phi(z)dz} \\ & \leq C \lim_{\beta_0 \rightarrow \infty} \frac{\int_{S\sqrt{\frac{K}{K-k_1}}\beta_0 - \sqrt{\frac{k_1}{K-k_1}}\beta_0}^{\infty} \phi(\beta_0)\phi(z)dz + \int_{\beta_0}^{\infty} \phi(z)\phi(S\sqrt{\frac{K}{K-k_1}}\beta_0 - \sqrt{\frac{k_1}{K-k_1}}z)dz}{\phi(S\beta_0)} \quad (\text{L'Hopital's rule}) \\ & \leq C \lim_{\beta_0 \rightarrow \infty} \left[\exp\left\{-\frac{\beta_0^2}{2}\left(S\sqrt{\frac{k_1}{K-k_1}} - \sqrt{\frac{K}{K-k_1}}\right)^2\right\} + \int_{\beta_0}^{\infty} \exp\left\{-\frac{1}{2}\left(\sqrt{\frac{K}{K-k_1}}z - S\sqrt{\frac{k_1}{K-k_1}}\beta_0\right)^2\right\}dz \right] = 0, \end{aligned}$$

Where $S = \sqrt{\frac{1}{b(1-r_1)}}$

(iii). When $c_2 \in \mathcal{D}_m$, given

$$\begin{aligned} 0 &= \frac{d}{dc_2} \frac{P(\sqrt{\frac{k_1}{K}}Z_1 + \sqrt{\frac{K-k_1}{K}}Z_2 > c_2, Z_1 > \beta_0)}{P(\sqrt{\frac{k_1}{K}}Z_1 + \sqrt{\frac{K-k_1}{K}}Z_2 > c_2)} \\ &= \frac{1}{P(\sqrt{\frac{k_1}{K}}Z_1 + \sqrt{\frac{K-k_1}{K}}Z_2 > c_2)^2} \times \\ & \quad \left\{ P(\sqrt{\frac{k_1}{K}}Z_1 + \sqrt{\frac{K-k_1}{K}}Z_2 > c_2) \frac{d}{dc_2} P(\sqrt{\frac{k_1}{K}}Z_1 + \sqrt{\frac{K-k_1}{K}}Z_2 > c_2, Z_1 > \beta_0) \right. \\ & \quad \left. - P(\sqrt{\frac{k_1}{K}}Z_1 + \sqrt{\frac{K-k_1}{K}}Z_2 > c_2, Z_1 > \beta_0) \frac{d}{dc_2} P(\sqrt{\frac{k_1}{K}}Z_1 + \sqrt{\frac{K-k_1}{K}}Z_2 > c_2) \right\} \end{aligned}$$

We have

$$\frac{P(\sqrt{\frac{k_1}{K}}Z_1 + \sqrt{\frac{K-k_1}{K}}Z_2 > c_2, Z_1 > \beta_0)}{P(\sqrt{\frac{k_1}{K}}Z_1 + \sqrt{\frac{K-k_1}{K}}Z_2 > c_2)} = \frac{\frac{d}{dc_2} P(\sqrt{\frac{k_1}{K}}Z_1 + \sqrt{\frac{K-k_1}{K}}Z_2 > c_2, Z_1 > \beta_0)}{\frac{d}{dc_2} P(\sqrt{\frac{k_1}{K}}Z_1 + \sqrt{\frac{K-k_1}{K}}Z_2 > c_2)}$$

Therefore,

$$\begin{aligned}
& \sup_{c_2 \in \mathcal{D}_m} \frac{P(\sqrt{\frac{k_1}{K}} Z_1 + \sqrt{\frac{K-k_1}{K}} Z_2 > c_2, Z_1 > \beta_0)}{P(\sqrt{\frac{k_1}{K}} Z_1 + \sqrt{\frac{K-k_1}{K}} Z_2 > c_2)} \\
&= \sup_{c_2 \in \mathcal{D}_m} \frac{\frac{d}{dc_2} P(\sqrt{\frac{k_1}{K}} Z_1 + \sqrt{\frac{K-k_1}{K}} Z_2 > c_2, Z_1 > \beta_0)}{\frac{d}{dc_2} P(\sqrt{\frac{k_1}{K}} Z_1 + \sqrt{\frac{K-k_1}{K}} Z_2 > c_2)} \\
&= \sup_{c_2 \in \mathcal{D}_m} C \int_{\beta_0}^{\infty} \exp \left\{ -\frac{1}{2} \left(\sqrt{\frac{K}{K-k_1}} z - \sqrt{\frac{k_1}{K-k_1}} c_2 \right)^2 \right\} dz \\
&\leq C \int_{\beta_0}^{\infty} \exp \left\{ -\frac{1}{2} \left(\sqrt{\frac{K}{K-k_1}} z - \sqrt{\frac{k_1}{K-k_1}} \gamma_m \right)^2 \right\} dz \\
&\rightarrow 0
\end{aligned}$$

Combine (i), (ii) and (iii), we have

$$\lim_{m \rightarrow \infty} \sup_{\mathcal{M}_1 \in \mathfrak{M}} \sup_{\substack{c_1 \in [\beta_0, \gamma_m] \\ c_2 \in [0, \gamma_m]}} \frac{P(\frac{1}{\sqrt{K}} \sum_{i=1}^K Z_i > c_2 | \frac{1}{\sqrt{|\mathcal{M}_1|}} \sum_{j \in \mathcal{M}_1} Z_j > c_1)}{P(\frac{1}{\sqrt{K}} \sum_{i=1}^K Z_i > c_2)} = 0$$

(2)

It is suffice to show

$$\lim_{m \rightarrow \infty} \sup_{\mathcal{M}_1 \in \mathfrak{M}} \sup_{c_2 \in [0, \bar{\Phi}^{-1}(1/m)]} \frac{P(\frac{1}{\sqrt{K}} \sum_{i=1}^K X_i > c_2, \frac{1}{\sqrt{|\mathcal{M}_1|}} \sum_{j \in \mathcal{M}_1} X_j > \beta_0)}{P(\sum_{i=1}^K Z'_i / \sqrt{K} > c_2)} \leq 0$$

Let $\check{X}_1 = \sum_{i \in \mathcal{M}_1} X_i / \sqrt{k_1}$, $\check{X}_2 = \sum_{i \in \mathfrak{M} \setminus \mathcal{M}_1} X_i / \sqrt{K - k_1}$.

Based on lemma 2, $\delta_{6m} = |P(\check{X}_j > p) / P(Z_j > p) - 1| \rightarrow 0$ uniformly for $j = 1, 2$ and $p > \alpha_m$.

Thus, uniformly,

$$\begin{aligned}
& P\left(\sqrt{\frac{k_1}{K}}\check{X}_1 + \sqrt{\frac{K-k_1}{K}}\check{X}_2 > c_2, \check{X}_1 > \beta_0\right) \\
&= P\left(\sqrt{\frac{K-k_1}{K}}\check{X}_2 > c_2 - \sqrt{\frac{k_1}{K}}\beta_0, \check{X}_1 > \beta_0\right) \\
&\quad + P\left(\sqrt{\frac{K-k_1}{K}}\check{X}_2 < c_2 - \sqrt{\frac{k_1}{K}}\beta_0, \sqrt{\frac{k_1}{K}}\check{X}_1 + \sqrt{\frac{K-k_1}{K}}\check{X}_2 > c_2\right) \\
&\leq (1 + \delta_{6m}) \left[P\left(\sqrt{\frac{K-k_1}{K}}\check{X}_2 > c_2 - \sqrt{\frac{k_1}{K}}\beta_0, Z_1 > \beta_0\right) \right. \\
&\quad \left. + P\left(\sqrt{\frac{K-k_1}{K}}\check{X}_2 < c_2 - \sqrt{\frac{k_1}{K}}\beta_0, \sqrt{\frac{k_1}{K}}Z_1 + \sqrt{\frac{K-k_1}{K}}\check{X}_2 > c_2\right) + P(Z_1 > \bar{\Phi}^{-1}(\alpha_m)) \right] \\
&\leq (1 + \delta_{6m})^2 \left[P\left(\sqrt{\frac{k_1}{K}}Z_1 + \sqrt{\frac{K-k_1}{K}}Z_2 > c_2, Z_1 > \beta_0\right) \right] + (1 + \delta_{6m}) \sum_{j=1}^2 P(Z_j > \bar{\Phi}^{-1}(\alpha_m)) \\
&\leq (1 + \delta_{6m})^2 \left[P\left(\sqrt{\frac{k_1}{K}}Z_1 + \sqrt{\frac{K-k_1}{K}}Z_2 > c_2, Z_1 > \beta_0\right) \right] + 2(1 + \delta_{6m})\alpha_m \\
&\leq o\left(P\left(\sum_{i=1}^K Z'_i/\sqrt{K} > c_2\right)\right)
\end{aligned}$$

□

Proof of Lemma 4. (i) Prove that (1) can leads to (2):

On $\cap_{t=1}^{\ell} \mathcal{X}^{(t)}$,

$$\sum_{S \in \mathcal{B}_0^{(\ell)}} |S| I(T_S < \hat{t}^{(\ell)}) \leq \sum_{S \in \mathcal{B}_0^{(\ell)}} |S| \hat{t}^{(\ell)} + \left\{ \sum_{S \in \mathcal{B}_0^{(\ell)}} |S| \hat{t}^{(\ell)} \right\} \epsilon$$

Combined with

$$\sum_{S \in \mathcal{B}_0^{(\ell)}} |S| \hat{t}^{(\ell)} \leq \alpha \sum_{S \in \mathcal{B}^{(\ell)}} |S| \mathbb{I}\{T_S < \hat{t}^{(\ell)}\}$$

and

$$\begin{aligned}
\sum_{S \in \mathcal{B}^{(\ell)}} |S| \mathbb{I}\{T_S < \hat{t}^{(\ell)}\} &= \sum_{S \in \mathcal{B}_0^{(\ell)}} |S| \mathbb{I}\{T_S < \hat{t}^{(\ell)}\} + \sum_{S \in \mathcal{B}_1^{(\ell)}} |S| \mathbb{I}\{T_S^{(\ell)} \leq \hat{t}^{(\ell)}\} \\
&\leq \sum_{S \in \mathcal{B}_0^{(\ell)}} |S| \mathbb{I}\{T_S^{(\ell)} < \hat{t}^{(\ell)}\} + Cm^{r_1}
\end{aligned}$$

We have:

$$(1 - \alpha - \alpha\epsilon) \sum_{S \in \mathcal{B}_0^{(\ell)}} |S| \hat{t}^{(\ell)} \leq \alpha C m^{r_1}$$

Thus, $2|\mathcal{B}_0^{(\ell)}| \hat{t}^{(\ell)} \leq \sum_{S \in \mathcal{B}_0^{(\ell)}} |S| \hat{t}^{(\ell)} \leq \frac{\alpha}{1 - \alpha - \alpha\epsilon} m^{r_1}$, for any $1 \leq \ell \leq L$.

When $\ell = 1$, by $|\mathcal{B}_0^{(1)}| = m_0 = m(1 + o(1))$, we have $\hat{t}^{(\ell)} \leq C m^{(r_1-1)}$.

When $\ell \geq 2$, on $\cap_{k=1}^{(\ell)} \mathcal{X}^{(k)}$, we have

$$\max_{k=1, \dots, \ell} \{FDP^{(k)} - \alpha\} < \epsilon$$

which leads to $|\mathcal{B}_0^{(\ell)}|/|\mathcal{B}^{(\ell)}| \rightarrow 1$. And accordingly, $\hat{t}^{(\ell)} \leq C m^{(r_1-1)}$.

(ii) Prove that statement (2) leads to statement (3)

On layer 1, $\bar{\Phi}(\hat{c}_S) = \hat{t}^{(1)} \leq C(m)^{r_1-1}$. On layer $\ell \geq 2$ and $\cap_{h=1}^{\ell} \mathcal{X}^{(h)}$, for all $S \in \mathcal{B}^{(\ell)}$,

$$\bar{\Phi}(\hat{c}_S) \leq G_S(\hat{c}_S) + \sum_{S' \in \mathcal{U}(S)} \bar{\Phi}(\hat{c}_{S'}) \quad (\text{S2})$$

Suppose $\bar{\Phi}(\hat{c}_{S'}) \leq C(m)^{r_1-1}$ for $S' \in \cup_{k=1}^{\ell-1} \mathcal{B}^{(k)}$, then together with $G_S(\hat{c}_S) = \hat{t}^{(\ell)} \leq C m^{r_1-1}$ and (S2), we have

$$\hat{c}_S \geq \sqrt{2(1 - r_1) \log m - 2 \log \log m} = \beta_m$$

for all $S \in \mathcal{B}^{(\ell)}$.

In addition, for $S \in \mathcal{B}^{(\ell)}$, on $\cap_{h=1}^{\ell-1} \mathcal{X}^{(h)}$,

$$G_S(\hat{c}_S) [1 - \bar{\Phi}(\frac{\beta_0}{\sqrt{M^{L-1}}})]^{M^{L-1}} \leq \bar{\Phi}(\hat{c}_S) \quad (\text{S3})$$

So we have $\bar{\Phi}(\hat{c}_S) \geq \hat{t}^{(\ell)}(1 + o(1))$, and accordingly, $\hat{c}_S \leq \gamma_m$.

Note that the $\hat{c}_S \leq \gamma_m$ only depends on the statement (2) on layer $\ell - 1$. Thus, we can apply the conclusion to show $P(m_0 \hat{t}^{(\ell)} > c \log m) \rightarrow 1$ in the proof of theorem 1.

(iii) Prove that statement (1) holds on layer 1 ($\ell = 1$):

Define $\nu_m = [(|\mathcal{A}'|^2/m + \delta_{2m}) \vee 1]/\sqrt{c_{\text{md}} \log m}$. Let $0 = c_0 < \dots < c_{\lceil \gamma_m/\nu_m \rceil} = \gamma_m$ satisfy

$c_k - c_{k-1} = \nu_m$ for $1 \leq k < \lceil \gamma_m / \nu_m \rceil$ and $c_{\lceil \gamma_m / \nu_m \rceil} - c_{\lceil \gamma_m / \nu_m \rceil - 1} \leq \nu_m$. We can get the corresponding p-values sequence $q_0 > \dots > q_{\lceil \gamma_m / \nu_m \rceil}$ with $q_k = 1 - \Phi(c_k)$. Let value $q^{(1)} = C^{(1)} c_{\text{md}} / m$, by (23), we have $P(\hat{t} > q^{(1)}) \rightarrow 1$. We define the working p-value sequence on layer 1 as $P_{sub}^{(1)} = \{q_0, \dots, q_{k^{(1)}}, q^{(1)}\}$, where $k^{(1)} \in \{0, \dots, \lceil \gamma_m / \nu_m \rceil - 1\}$ is the index s.t. $q_{k^{(1)}} \geq q^{(1)}$ and $q_{k^{(1)}+1} \leq q^{(1)}$.

If $\forall \epsilon > 0$,

$$P\left(\max_{q \in P_{sub}^{(1)}} \left| \frac{\sum_{S \in \mathcal{B}_0^{(1)}} I(X_S > \bar{\Phi}^{-1}(q)) - \sum_{S \in \mathcal{B}_0^{(1)}} P(X_S > \bar{\Phi}^{-1}(q))(1 - \delta_{0m})}{\sum_{S \in \mathcal{B}_0^{(1)}} q} \right| > \epsilon \right) \rightarrow 0 \quad (\text{S4})$$

Then,

$$\begin{aligned} & P\left(\max_{q \in P_{sub}^{(1)}} \frac{\sum_{S \in \mathcal{B}_0^{(1)}} I(T_S^{(1)} < q) - \sum_{S \in \mathcal{B}_0^{(1)}} q}{\sum_{S \in \mathcal{B}_0^{(1)}} q} > \epsilon\right) \\ & \leq P\left(\max_{q \in P_{sub}^{(1)}} \frac{\sum_{S \in \mathcal{B}_0^{(1)}} I(X_S > \bar{\Phi}^{-1}(q)) - \sum_{S \in \mathcal{B}_0^{(1)}} P(\tilde{X}_S > \bar{\Phi}^{-1}(q))}{\sum_{S \in \mathcal{B}_0^{(1)}} q} > \epsilon\right) \\ & \leq P\left(\max_{q \in P_{sub}^{(1)}} \frac{\sum_{S \in \mathcal{B}_0^{(1)}} I(X_S > \bar{\Phi}^{-1}(q)) - \sum_{S \in \mathcal{B}_0^{(1)}} P(X_S > \bar{\Phi}^{-1}(q))(1 - \delta_{0m})}{\sum_{S \in \mathcal{B}_0^{(1)}} q} > \epsilon\right) \\ & \leq P\left(\max_{q \in P_{sub}^{(1)}} \left| \frac{\sum_{S \in \mathcal{B}_0^{(1)}} I(X_S > \bar{\Phi}^{-1}(q)) - \sum_{S \in \mathcal{B}_0^{(1)}} P(X_S > \bar{\Phi}^{-1}(q))(1 - \delta_{0m})}{\sum_{S \in \mathcal{B}_0^{(1)}} q} \right| > \epsilon\right) \\ & = o(1) \end{aligned} \quad (\text{S5})$$

Together with the fact that $\sup_{j=1, \dots, k} |q_{(j)} / q_{(j-1)} - 1| = o(1)$, we have

$$P\left(\sup_{q \in [q^{(1)}, \alpha]} \frac{\sum_{S \in \mathcal{B}_0^{(1)}} I(T_S < q) - \sum_{S \in \mathcal{B}_0^{(1)}} q}{\sum_{S \in \mathcal{B}_0^{(1)}} q} > \epsilon\right) = o(1)$$

Thus, to prove (1) holds on layer 1, we only need to show (S4).

Define $C_{sub}^{(1)} = \{c_0, \dots, c_{k'}, c'\}$, with $c' = \bar{\Phi}^{-1}(q')$. In order to show (S4), it is suffice to show

$$\int_0^{c'} P\left\{\left| \frac{\sum_{S \in \mathcal{B}_0^{(1)}} I(X_S > c) - P(X_S > c)(1 - \delta_{0m})}{\sum_{S \in \mathcal{B}_0^{(1)}} \bar{\Phi}(c)} \right| \geq \epsilon \right\} dc = o(\nu_m) \quad (\text{S6})$$

Note that by Markov inequality,

$$\begin{aligned}
& P \left\{ \left| \frac{\sum_{S \in \mathcal{B}_0^{(1)}} [I(X_S > c) - P(X_S > c)(1 - \delta_{0m})]}{\sum_{S \in \mathcal{B}_0^{(1)}} \bar{\Phi}(c)} \right| \geq \epsilon \right\} \\
& \leq P \left\{ \left| \frac{\sum_{S \in \mathcal{B}_0^{(1)}} [I(X_S > c) - P(X_S > c)]}{\sum_{S \in \mathcal{B}_0^{(1)}} \bar{\Phi}(c)} \right| \geq \epsilon - (1 + \delta_{0m})\delta_{0m} \right\} \\
& \leq \frac{\sum_{S, S' \in \mathcal{B}_0^{(1)}} [P(X_S > c, X_{S'} > c) - P(X_S > c)P(X_{S'} > c)]}{(\sum_{S \in \mathcal{B}_0^{(1)}} \bar{\Phi}(c))^2 [\epsilon - (1 + \delta_{0m})\delta_{0m}]^2}
\end{aligned}$$

We can divide the $S, S' \in \mathcal{B}_0^{(1)}$ into the following three subsets:

$$\begin{aligned}
\mathcal{B}_{01}^{(1)} &= \{S, S' \in \mathcal{B}_0^{(1)} : S = S'\} \\
\mathcal{B}_{02}^{(1)} &= \{S, S' \in \mathcal{B}_0^{(\ell)} : S \neq S', \exists A, A' \in \mathcal{A}^{(L)}, \text{ s.t. } S \subset A, S' \subset A', \text{ and } A' \in \Gamma_A\} \\
\mathcal{B}_{03}^{(1)} &= \{S, S' \in \mathcal{B}_0^{(1)} : S \neq S'\} \setminus \mathcal{B}_{02}^{(1)}
\end{aligned} \tag{S7}$$

Then,

$$\frac{\sum_{(S, S') \in \mathcal{B}_{01}^{(1)}} [P(X_S > c, X_{S'} > c) - P(X_S > c)P(X_{S'} > c)]}{(\sum_{S \in \mathcal{B}_0^{(1)}} \bar{\Phi}(c))^2 [\epsilon - (1 + \delta_{0m})\delta_{0m}]^2} \leq \frac{C}{\sum_{S \in \mathcal{B}_0^{(1)}} \bar{\Phi}(c)}$$

Based on condition 3,

$$\frac{\sum_{(S, S') \in \mathcal{B}_{02}^{(1)}} [P(X_S > c, X_{S'} > c) - P(X_S > c)P(X_{S'} > c)]}{(\sum_{S \in \mathcal{B}_0^{(1)}} \bar{\Phi}(c))^2 [\epsilon - (1 + \delta_{0m})\delta_{0m}]^2} \leq \frac{C(|\mathcal{A}'|^2/m + \delta_{2m})}{\sum_{S \in \mathcal{B}_0^{(1)}} \bar{\Phi}(c)}$$

In addition,

$$\frac{\sum_{(S, S') \in \mathcal{B}_{03}^{(1)}} [P(X_S > c, X_{S'} > c) - P(X_S > c)P(X_{S'} > c)]}{(\sum_{S \in \mathcal{B}_0^{(1)}} \bar{\Phi}(c))^2 [\epsilon - (1 + \delta_{0m})\delta_{0m}]^2} = o(1)$$

Thus, after some calculation, we can prove (S6) and then $P(\mathcal{X}^{(1)}) \rightarrow 1$.

Similarly, if $|\tilde{\Omega}_0| = m(1 + o(1))$, based on (S4), we have

$$P \left(\max_{q \in P_{sub}^{(1)}} \left| \frac{\sum_{S \in \mathcal{B}_0^{(1)}} I(T_S^{(1)} < q) - \sum_{S \in \mathcal{B}_0^{(1)}} q}{\sum_{S \in \mathcal{B}_0^{(1)}} q} \right| > \epsilon \right) = o(1)$$

Hence, $P(\mathcal{X}'^{(1)}) \rightarrow 1$.

(iv) Prove that statement (1) holds on layer $\ell \geq 2$ when statement (1) holds on previous layers:

On layer ℓ , we can divide the $S, S' \in \mathcal{B}_0^{(\ell)}$ into the following three subsets:

$$\mathcal{B}_{01}^{(\ell)} = \{S, S' \in \mathcal{B}_0^{(\ell)} : S = S', \{T_i : i \in S\} \text{ are mutually independent}\}$$

$$\mathcal{B}_{02}^{(\ell)} = \{S, S' \in \mathcal{B}_0^{(\ell)} : \exists A, A' \in \mathcal{A}^{(L)}, \text{ s.t. } S \subset A, S' \subset A', \text{ and } A' \in \Gamma_A\}$$

$$\mathcal{B}_{03}^{(\ell)} = \{S, S' \in \mathcal{B}_0^{(\ell)} : S \neq S'\} \setminus \mathcal{B}_{02}^{(\ell)}$$

Consider the p-values sequence $q_0 > \dots > q_{\lceil \gamma_m / \nu_m \rceil}$ constructed in (iii). Let $q^{(\ell)} = C^{(\ell)} c_{\text{md}} / m$, by (23), we have $P(\hat{t} > q^{(\ell)}) \rightarrow 1$. We define the working p-value sequence on layer 1 as $P_{\text{sub}}^{(\ell)} = \{q_0, \dots, q_{k^{(\ell)}}, q^{(\ell)}\}$, where $k^{(\ell)} \in \{0, \dots, \lceil \gamma_m / \nu_m \rceil - 1\}$ is the index s.t. $q_{k^{(\ell)}} \geq q^{(\ell)}$ and $q_{k^{(\ell)}+1} \leq q^{(\ell)}$.

In view of statement (3) and Lemma 3, we have

$$\sup_{k=0, \dots, \lceil \gamma_m / \nu_m \rceil} \left| \frac{G_S(c_k)}{\bar{\Phi}(c_k)} - 1 \right| = o(1)$$

Together with statement (3) and Lemma 2, there exists $\delta_5(m) \rightarrow 0$ with

$$\begin{aligned} & \max_{S \in \mathcal{B}_0^{(\ell)}} \frac{P(X_S > \bar{\Phi}^{-1}(q) | \mathcal{Q}^{(1:\ell-1)})}{q} \\ & \leq \max_{S \in \mathcal{B}_0^{(\ell)}} \frac{P(X_S > \bar{\Phi}^{-1}(q))}{P(Z_S > \bar{\Phi}^{-1}(q)) [1 - \bar{\Phi}(\frac{\beta_0}{\sqrt{M^{L-1}}})]^{M^{L-1}}} \\ & \leq 1 + \delta_5(m) \end{aligned}$$

Then $\forall \epsilon > 0$, by following the similar arguments in (iii), we can have

$$\begin{aligned} & P\left(\max_{q \in P_{\text{sub}}^{(\ell)}} \left| \frac{\sum_{S \in \mathcal{B}_{01}^{(\ell)}} |S| I(X_S > \bar{\Phi}^{-1}(q)) - \sum_{S \in \mathcal{B}_{01}^{(\ell)}} |S| P(X_S > \bar{\Phi}^{-1}(q) | \mathcal{Q}^{(1:\ell-1)}) (1 + \delta_{0m})}{\sum_{S \in \mathcal{B}_{01}^{(\ell)}} |S| q} \right| > \epsilon \middle| \mathcal{Q}^{(1:\ell-1)} \right) \\ & \rightarrow 0 \end{aligned} \tag{S8}$$

Then,

$$\begin{aligned}
& P\left(\max_{q \in P_{sub}^{(\ell)}} \frac{\sum_{S \in \mathcal{B}_0^{(\ell)}} |S| I(T_S < q) - \sum_{S \in \mathcal{B}_0^{(\ell)}} |S| q}{\sum_{S \in \mathcal{B}_0^{(\ell)}} |S| q} > \epsilon \middle| \mathcal{Q}^{(1:\ell-1)}\right) \\
& \leq P\left(\max_{q \in P_{sub}^{(\ell)}} \frac{\sum_{S \in \mathcal{B}_0^{(\ell)}} |S| I(X_S > \bar{\Phi}^{-1}(q)) - \sum_{S \in \mathcal{B}_0^{(\ell)}} |S| P(X_S > \bar{\Phi}^{-1}(q)) \mathcal{Q}^{(1:\ell-1)}}{\sum_{S \in \mathcal{B}_0^{(\ell)}} |S| q} > \epsilon/2 \middle| \mathcal{Q}^{(1:\ell-1)}\right) \\
& = o(1) \tag{S9}
\end{aligned}$$

Together with the fact that $\sup_{j=1, \dots, k} |q_{(j)}/q_{(j-1)} - 1| = o(1)$, we have

$$P\left(\sup_{q \in [q^{(\ell)}, \alpha]} \frac{\sum_{S \in \mathcal{B}_0^{(\ell)}} |S| I(T_S < q) - \sum_{S \in \mathcal{B}_0^{(\ell)}} |S| q}{\sum_{S \in \mathcal{B}_0^{(\ell)}} |S| q} > \epsilon \middle| \mathcal{Q}^{(1:\ell-1)}\right) = o(1)$$

And thus $P(\mathcal{X}^{(\ell)}) \rightarrow 1$.

Similarly, based on Lemma 3 (2), when $|\tilde{\Omega}_0| = m(1 + o(1))$, we have $P(\mathcal{X}'^{(\ell)}) \rightarrow 1$. \square

Proof of Lemma 5. When $\ell = 1$:

for $\delta = 1/m^4$,

$$\begin{aligned}
\sum_{S \in \mathcal{B}_0^{(1)}} |S| \hat{t}^{(1)} & \leq \alpha \sum_{S \in \mathcal{B}^{(1)}} |S| I(T_S < \hat{t}^{(1)}) \\
& \leq \alpha \sum_{S \in \mathcal{B}^{(1)}} |S| I(T_S < \hat{t}^{(1)} + \delta) \\
& \leq \sum_{S \in \mathcal{B}_0^{(1)}} |S| \hat{t}^{(1)} (1 + o(1)) \tag{S10}
\end{aligned}$$

Assume (19) holds on layer $1, \dots, \ell - 1$. Then,

$$\sum_{S \in \mathcal{B}_0^{(\ell)}} |S| \hat{t}^{(\ell)} \leq \alpha(1 + o(1)) \sum_{S \in \mathcal{B}^{(\ell)}} |S| I(T_S < \hat{t}^{(\ell)})$$

Thus, by following the similar arguments on (S10), we can get (19) on layer ℓ . \square